francesco.prudenzano@poliba.it

Principi di funzionamento e potenzialità delle fibre ottiche

Francesco Prudenzano

Infrastrutturazione del territorio con fibra ottica: opportunità di sviluppo sociale ed economico

Seminario Tecnico

Ordine degli Ingegneri della Provincia di Bari
AEIT - Sezione Pugliese
Collegio dei Periti Industriali delle Province di Bari e B.A.T.

14 novembre 2017 Aula Magna "E. Orabona"
Politecnico di Bari - Via Edoardo Orabona, 4 Bari

OVERVIEW

- Basic operation principle of optical fibers
- Recalls on optical fiber technology
- Guided modes in optical fibers
- Dispersion and Nonlinear phenomena in Optical Fibers (group velocity dispersion, material dispersion, waveguide dispersion. Propagation of optical pulses in an optical fiber, including all linear and nonlinear effects, described by nonlinear Schrödinger equation (NLSE). Supercontinuum (SC) generation)
- Active fiber devices: amplifiers and lasers.
- Fiber sensing: fiber Bragg grating, Long Period Grating, fiber tapers

FIBER OPTIC STRUCTURE

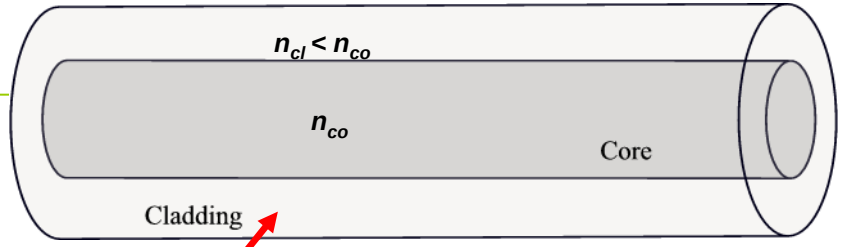

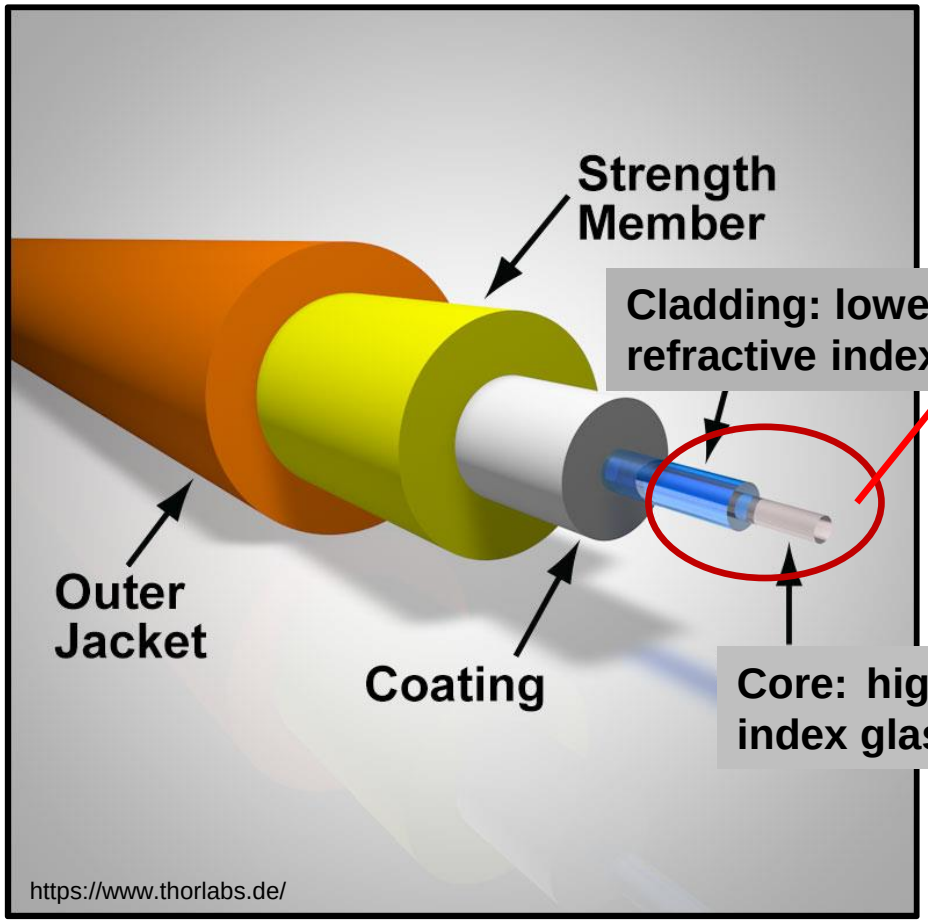

Tipycal size for single mode fiber
Core: 5-9 μm
Cladding: 125 μm
Coating: 170-250 μm

Human hair: 90 μm

MAXWELL'S EQUATION TO EXHAUSTIVELY AND EXACTLY MODEL.....RAY OPCTICS AND SNELL TO QUICKLY UNDERSTAND

$v = \frac{c}{n}$; c =3 x 10^8 m/s

$\theta_c = \arcsin\left(\frac{n_{cl}}{n_{co}}\right)$

$n_{co} \sin\theta_i = n_{cl} \sin\theta_t$

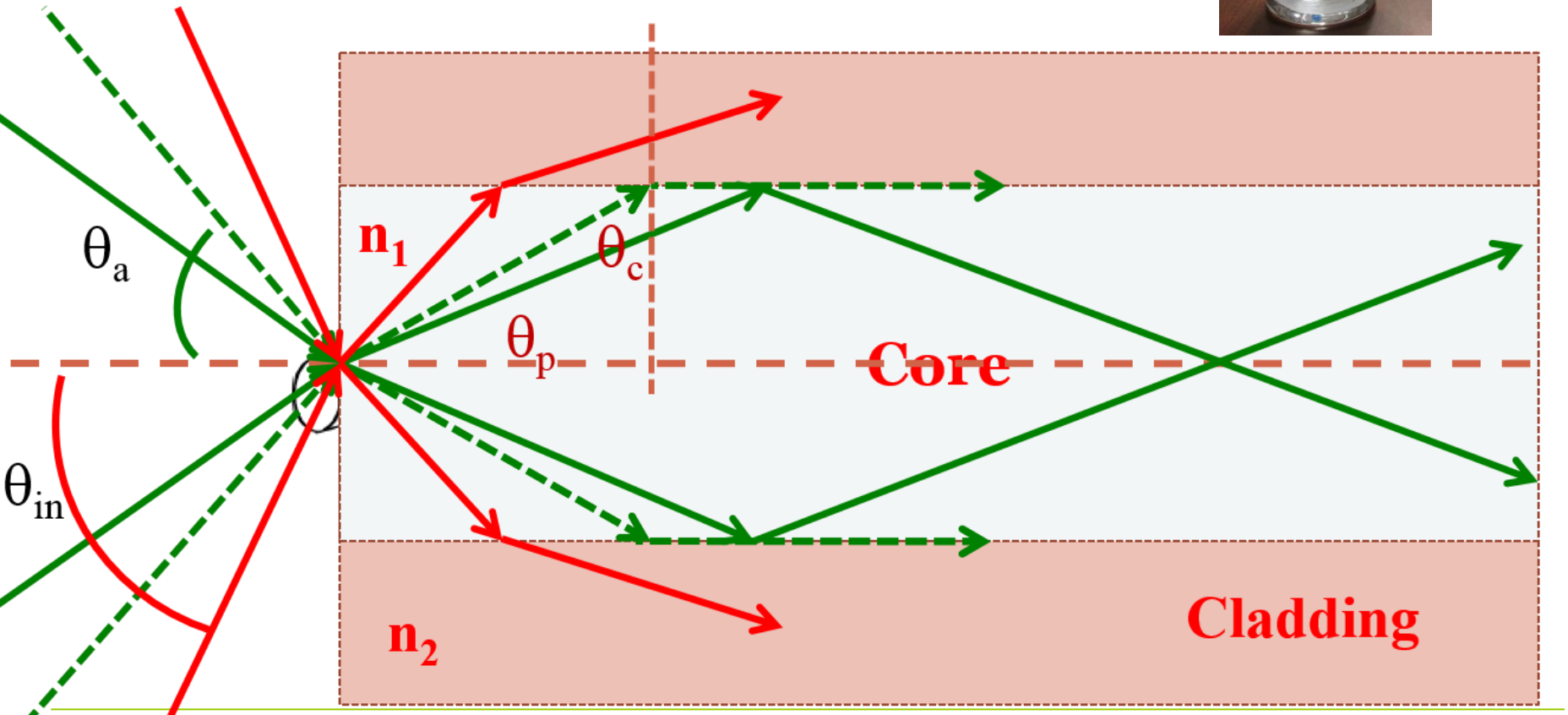

https://www.quora.com/

$$1 \cdot \sin\theta_a = n_{co} \sin\left(\frac{\pi}{2} - \theta_c\right) = n_{co}\sqrt{1 - \cos^2\left(\frac{\pi}{2} - \theta_c\right)}$$

$$\cos\left(\frac{\pi}{2} - \theta_c\right) = \sin\theta_c = \frac{n_{cl}}{n_{co}}$$

$$\sin\theta_a = n_{co}\sqrt{1 - \left(\frac{n_{cl}}{n_{co}}\right)^2} = \sqrt{n_{co}^2 - n_{cl}^2}$$

Fiber optic cables- How they work.mp4

$$\theta_a = \arcsin(N.A.)$$

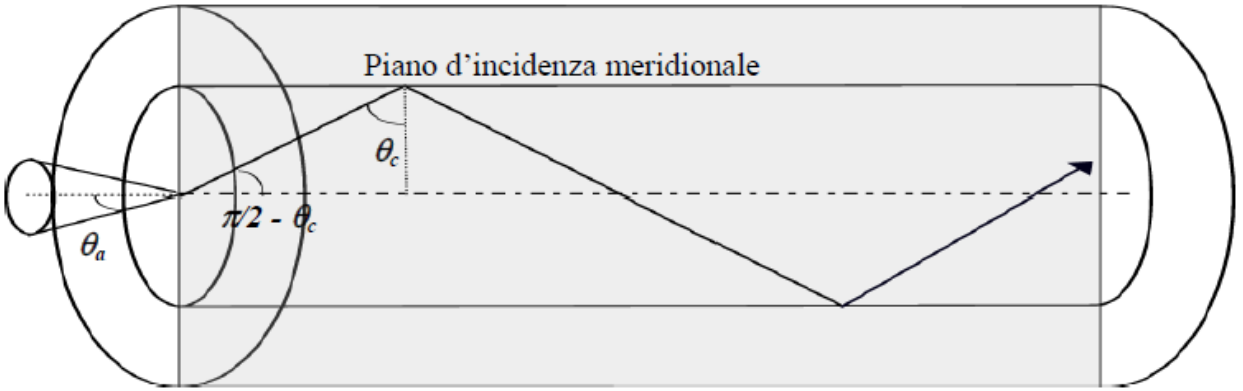

MODAL DISPERSION: different paths and refractive index dispersion

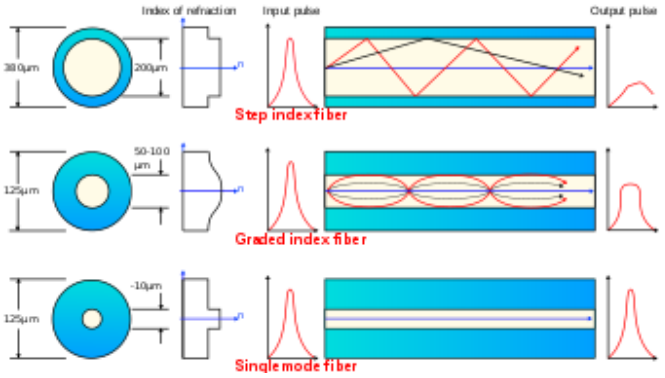

$$v_g = \frac{d\omega}{d\beta} \qquad n^2(r) = n_{co}^2\left[1 - 2\left(\frac{r}{a}\right)^p \Delta\right] \qquad \Delta = \frac{n_{co}^2 - n_{cl}^2}{2n_{co}^2} \cong \frac{n_{co} - n_{cl}}{n_{cl}}$$

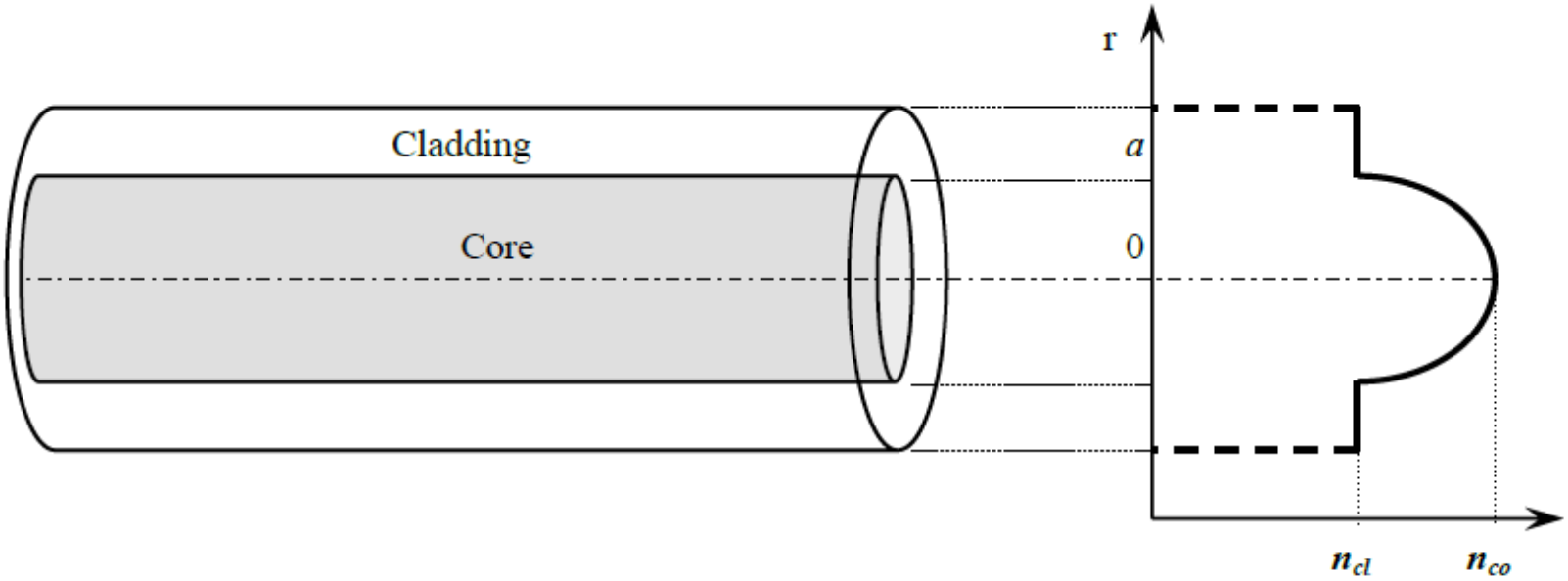

(a) Multimode step-index fiber

Various kinds of optical fibers.

Reference: Elements of Photonics, Volume II: For Fiber and Integrated Optics. Keigo Iizuka p 704
Moreover see you tube videos on basic principles

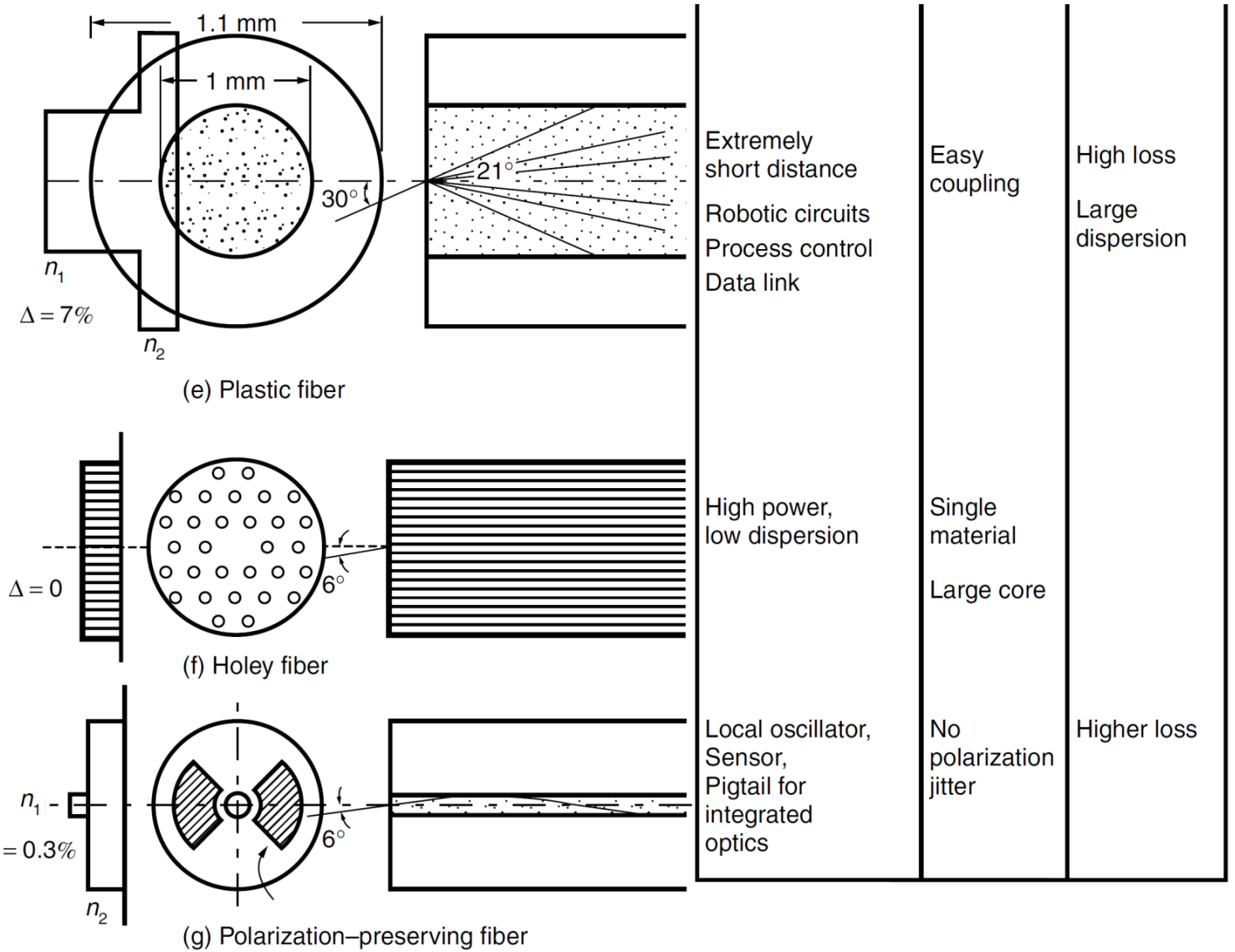

Guided propagation mode as Maxwell's equations solutions

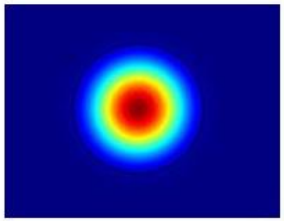

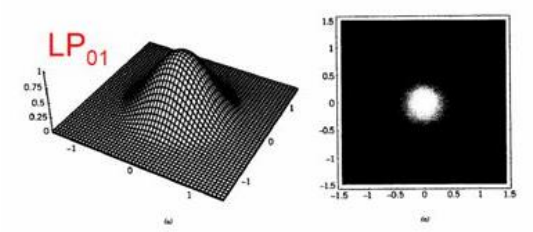

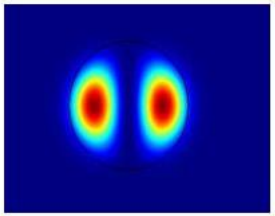

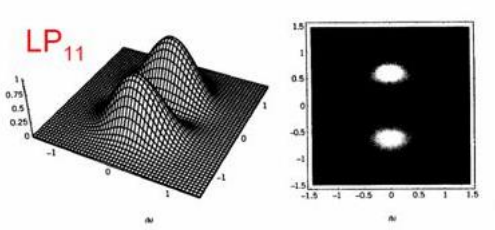

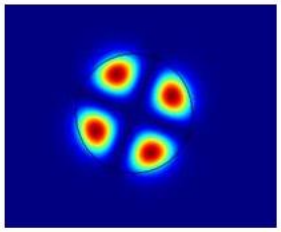

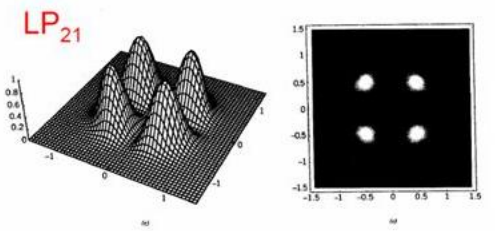

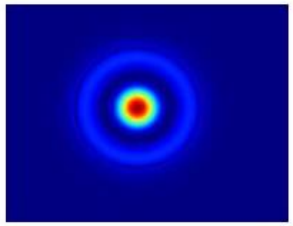

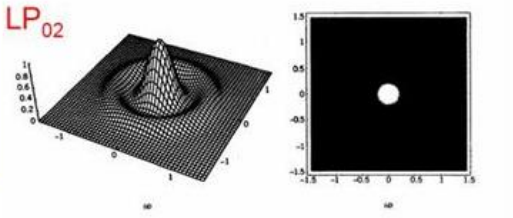

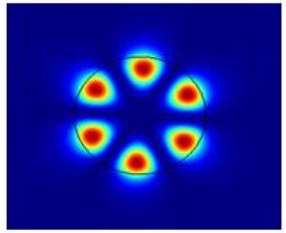

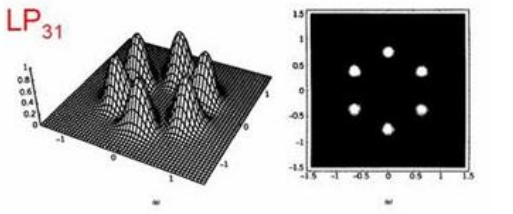

FABRICATION OF OPTICAL FIBERS

Reference: Elements of Photonics, Volume II: For Fiber and Integrated Optics. Keigo Iizuka, pp 775-783

Fabrication of optical fiber by the double-crucible method.

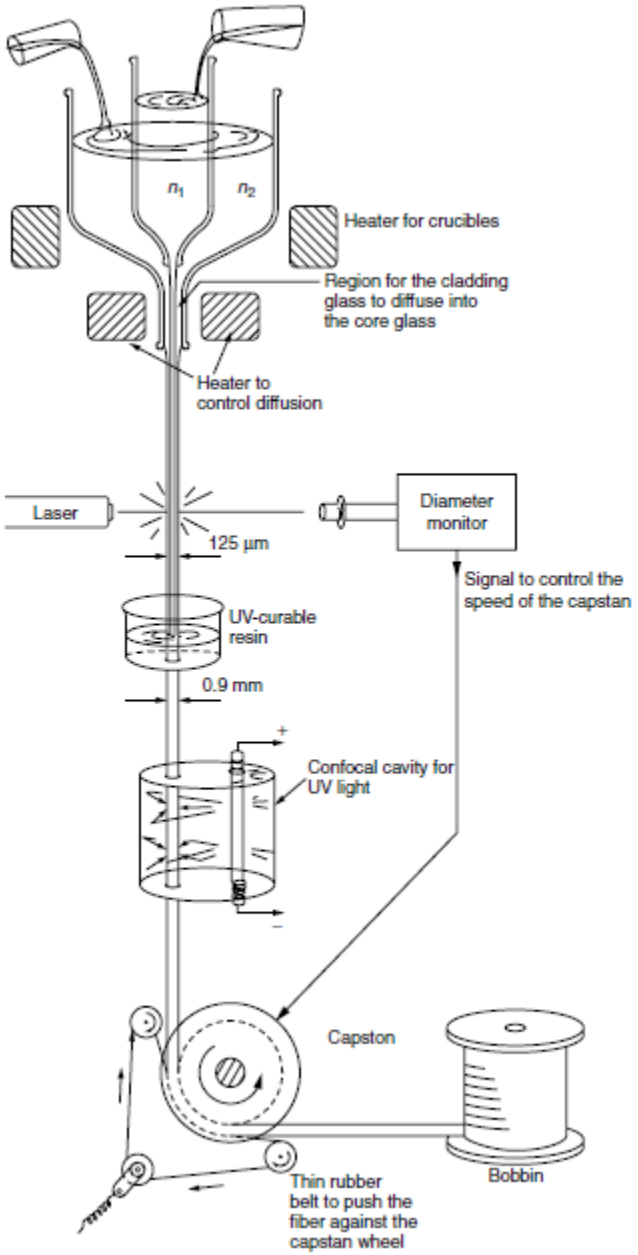

It is the **chemical vapor deposition (CVD)** method that possible to attain such a high degree of purity. The CVD method was originally developed in semiconductor industries. It is an extremely effective method. The method uses the difference in the vapor pressures of the liquid metal halides of the material and those of the impurities. Figure shows the vapor pressures of various metal halides as a function of temperature. Metal halides such as BCl_3, $SiCl_4$, and $POCl_3$ are used for the material, and VCl_4 and $FeCl_3$ are the impurities to be removed.

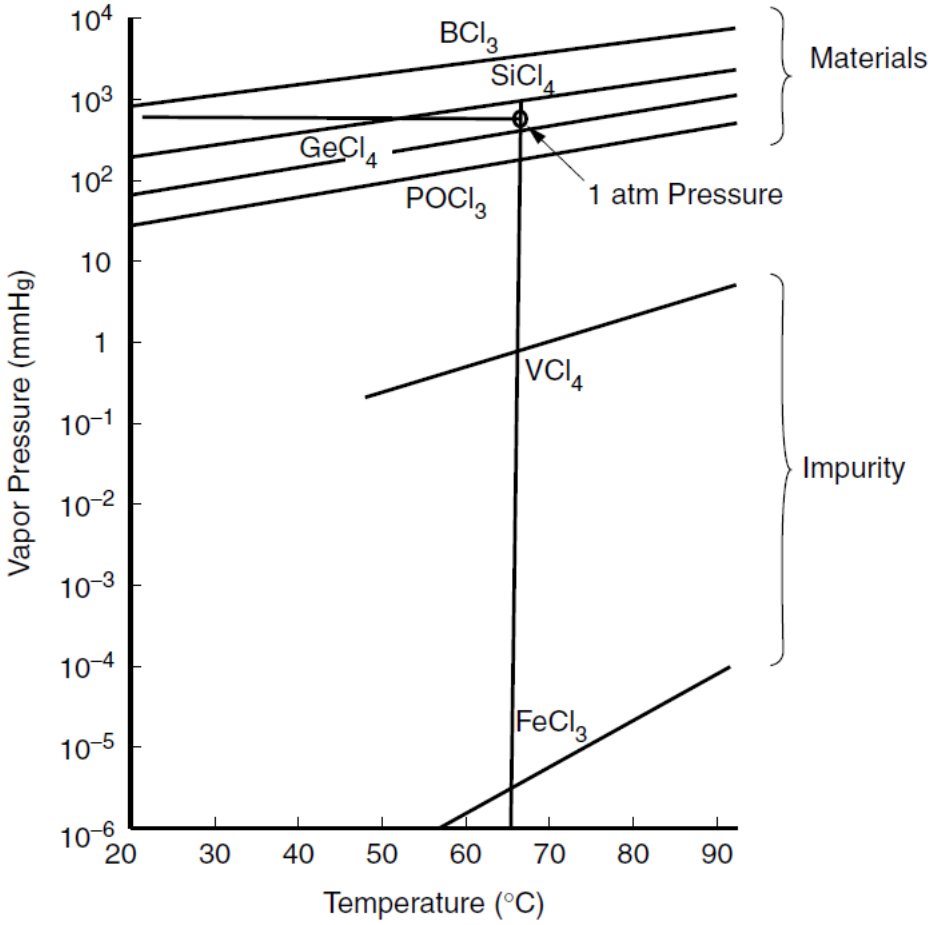

Relation of vapor pressures for metal halide additives and potential impurities. (After P. C. Schultz [48].)

Modified chemical vapor deposition (MCVD) method.

The MCVD arrangement is shown in Fig. The material gases are prepared by the CVD method. Material halides in liquid form, such as $SiCl_4$, $GeCl_4$, and $POCl_3$, are stored in separate reservoirs. Purified oxygen gas is bubbled into these reservoirs at a prescribed pressure and temperature so that only the pure material gas can bubble out. The bubbled out material gases are mixed in prescribed proportions and led into the inside of a silica tube. The mixture proportions are manipulated by a computer-controlled mass flow manifold.

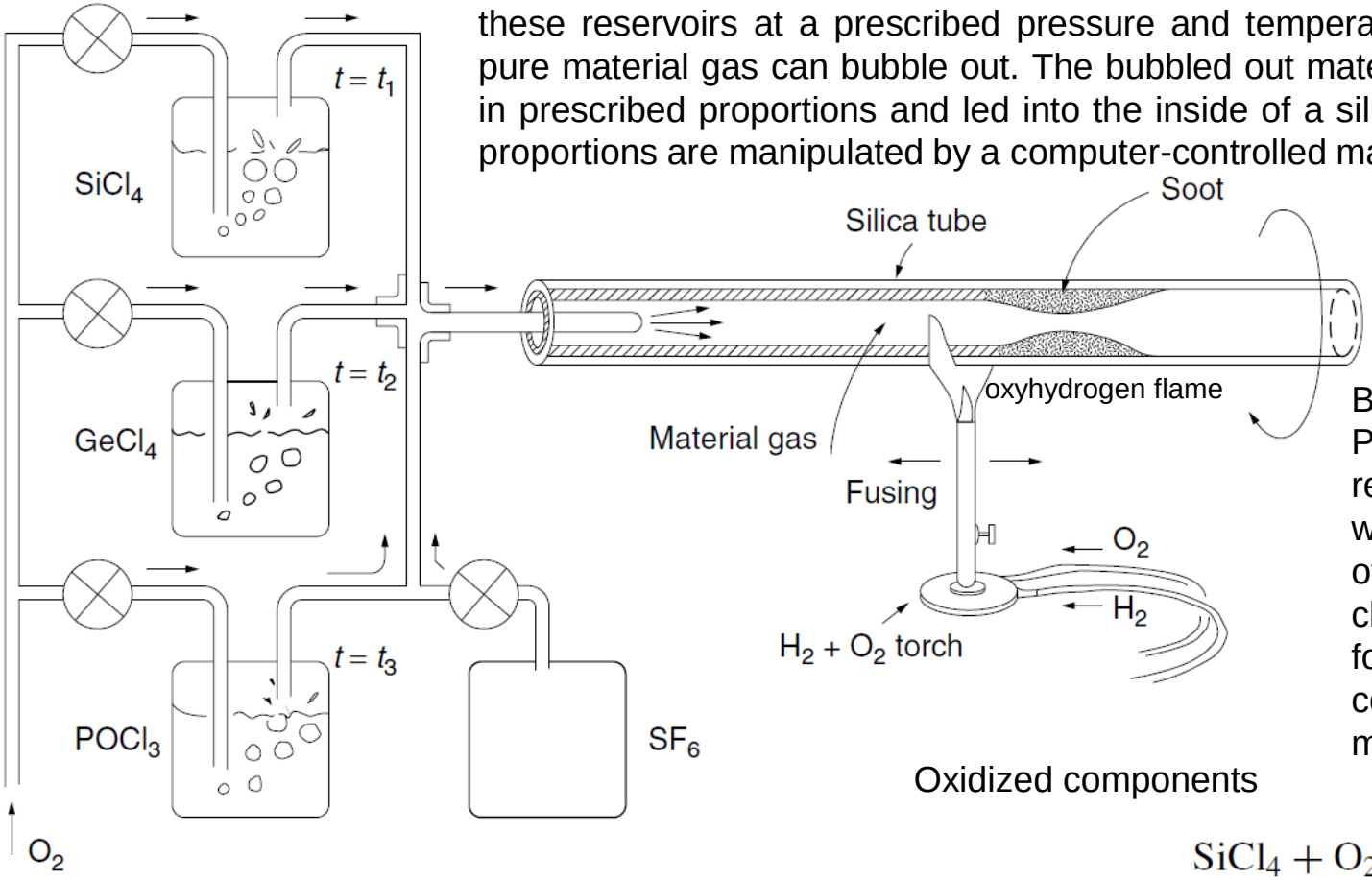

Both dopants GeO_2 and P_2O_5 raise the index of refraction of the glass, while F lowers the index of refraction. Core and cladding layers are formed by programmed control of the mass flow manifolds.

Oxidized components

$$SiCl_4 + O_2 \rightarrow SiO_2 + 2Cl_2$$

$$GeCl_4 + O_2 \rightarrow GeO_2 + 2Cl_2$$

$$4POCl_3 + 3O_2 \rightarrow 2P_2O_5 + 6Cl_2$$

The PCVD method uses the plasma generated in a microwave cavity instead of the oxyhydrogen flame as a source of heating. The cavity is cylindrical in shape and is resonated at a few gigahertz.

The material gas becomes direct-deposited new glass on the tube wall, instead of by way of soot. Advantages of the PCVD method over the MCVD method are that, in the PCVD method, the **deposition efficiency** and **speed are higher**, there is **greater control over profiles because the temperature can be more precisely controlled, and the tube need not be rotated.**

PMCVD is quite similar to PCVD except that it uses an induction heater operated at a few megahertz. The advantage of the induction heater over the microwave cavity is that it does not require a vacuum. The temperatures obtainable with the induction heater are not high enough to fuse the glass directly to the tube wall, so that the **process has to be assisted by an additional oxyhydrogen flame.**

Outside vapor deposition (OVD) method

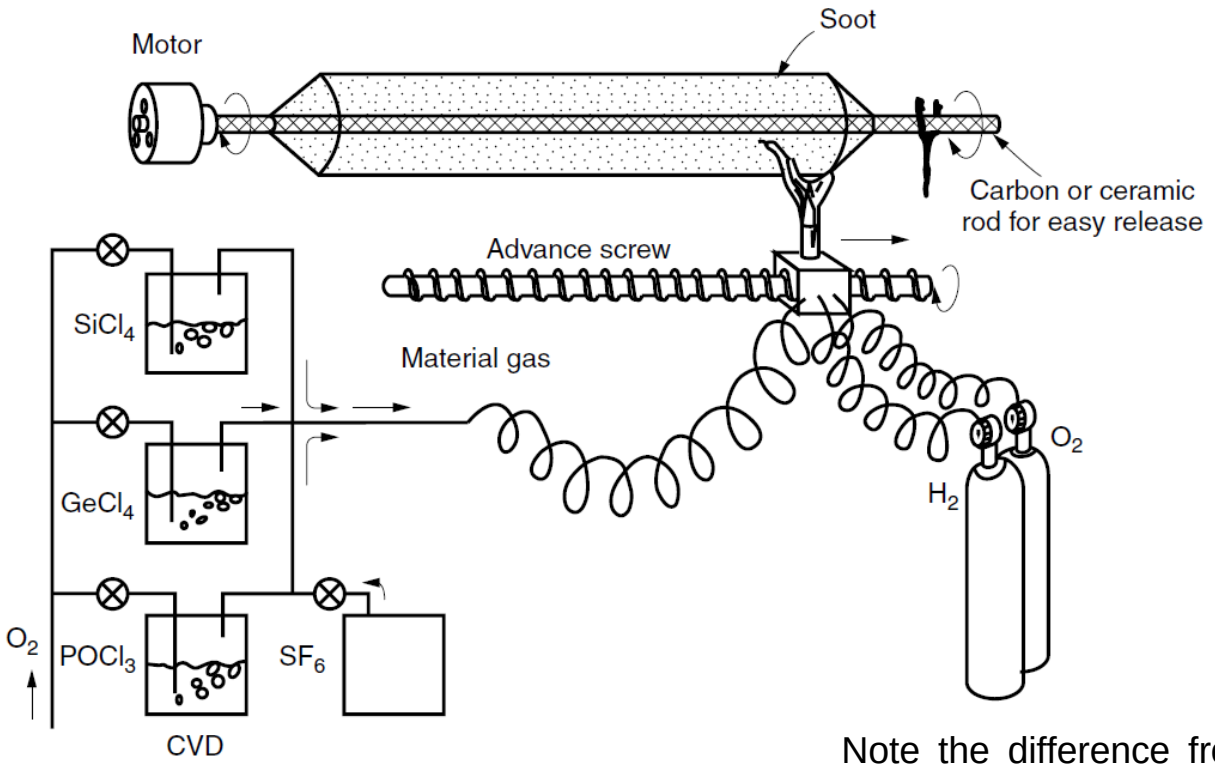

Note the difference from the case of MCVD where there is no chance that the material gases meet hydrogen.

$$GeCl_4 + O_2 + 2H_2 = GeO_2 + 4HCl$$

$$SiCl_4 + O_2 + 2H_2 = SiO_2 + 4HCl$$

Vapor-phase axial deposition (VAD) method.

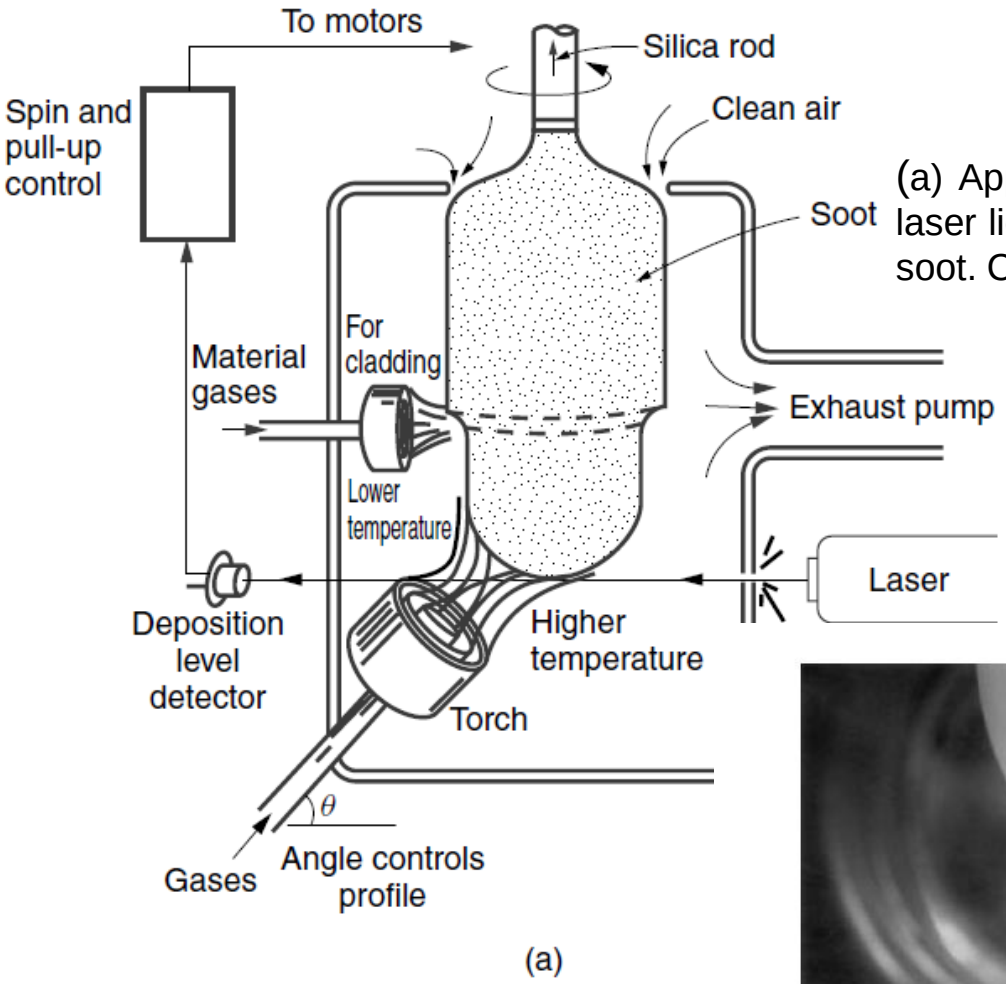

(a)

(a) Apparatus. (b) Deposit of the soot. Ahorizontal laser light monitors the position of the bottom of the soot. Courtesy of H. Murata).

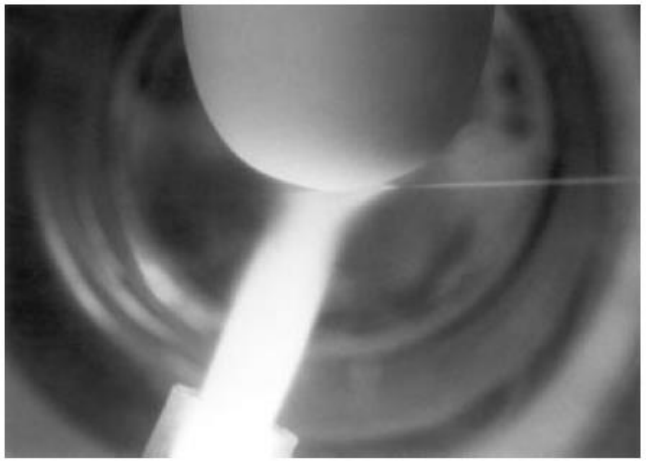

(b)

Apparatus for drawing a fiber

Preform is heated in a furnace to **2000–2100°C, which is a few hundred degrees above the melting temperature (1900°C) of the fiber.** The furnace makes it possible to draw an optical fiber with a specified diameter in one step. The furnace is made out of a fat **graphite filament bent** like a cage surrounding the preform. Argon gas is blown into the furnace so as to protect the filament from oxidation burnout

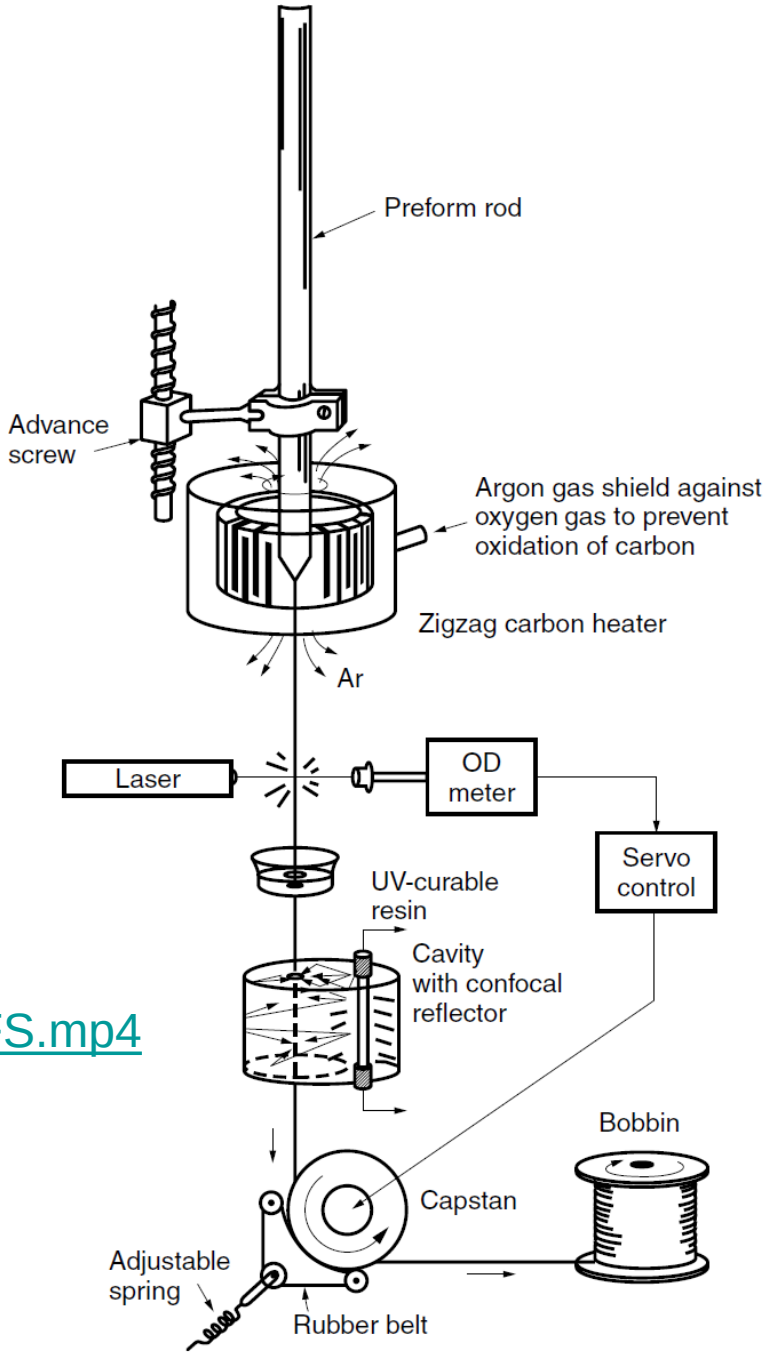

Manufacturing Multimode Optical Fiber at OFS.mp4

Fiber dispersion

References: Fiber optic Communication System, third Edition, G. P. Agraval - John Wiley & Sons pp 24-26, Lecture notes DEMONSTRATION_1

One can find the maximum angle that the incidentray should make with the fiber axis to remain confined inside the core.

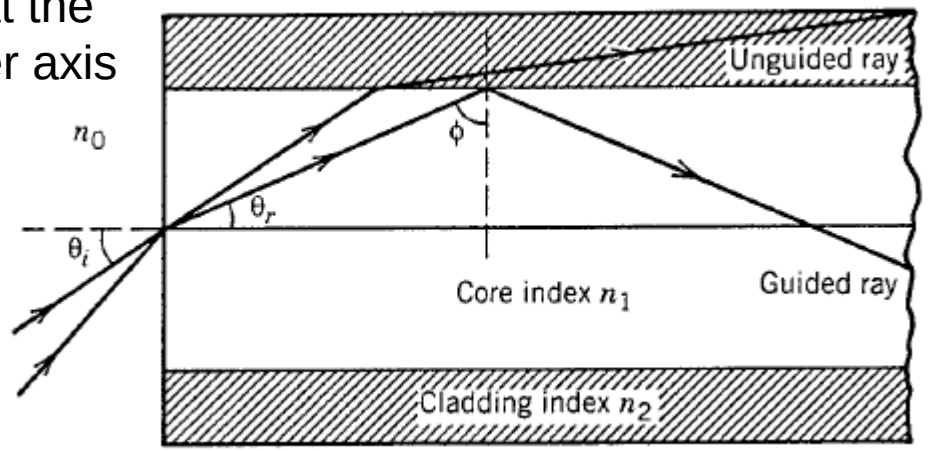

Multipath dispersion

$$n_0 \sin\theta_i = n_1 \sin\theta_r,$$

$$\sin\phi_c = n_2/n_1,$$

$$\theta_r = \pi/2 - \phi_c$$

$$n_0 \sin\theta_i = n_1 \cos\phi_c = (n_1^2 - n_2^2)^{1/2}.$$

$$\mathrm{NA} = n_1(2\Delta)^{1/2}$$

fractional index change at the core–cladding interface $\Delta = (n_1 - n_2)/n_1,$

The shortest path L occurs for $\theta_i = 0$

The longest path $L/\sin\phi_c.$

Dem.

time delay $$\Delta T = \frac{n_1}{c}\left(\frac{L}{\sin\phi_c} - L\right) = \frac{L}{c}\frac{n_1^2}{n_2}\Delta.$$

A short pulse (called an impulse) would broaden considerably as a result of different path lengths. One can estimate the extent of ulse broadening simply by considering the shortest and longest ray paths.

ΔT is related to the information-carrying capacity of the fiber measured through the bit rate B.

Δ*T* should be less than the allocated bit slot ($T_B = 1/B$). Thus, an order-of-magnitude estimate of the bit rate is obtained from the condition $B\Delta T < 1$.

$$BL < \frac{n_2}{n_1^2}\frac{c}{\Delta}.$$

As an illustration, consider an unclad glass fiber with $n_1 = 1.5$ and $n_2 = 1$. The bit rate–distance product of such a fiber is limited to quite small values since $BL < 0.4$ (Mb/s)-km. **Dem.**

Most fibers for communication applications are designed with Δ < 0.01

Such fibers can communicate data at a bit rate of 10 Mb/s over distances up to 10 km and may be suitable for some local-area networks.

References: Fiber optic Communication System, third Edition, G. P. Agraval - John Wiley & Sons pp 35-36, Lecture notes DEMONSTRATION_1

Fiber Birefringence

The degenerate nature of the orthogonally polarized modes holds only for an ideal single-mode fiber with a perfectly cylindrical core of uniform diameter. Real fibers exhibit considerable variation in the shape of their core along the fiber length. They may also experience nonuniform stress such that the cylindrical symmetry of the fiber is broken. Degeneracy between the orthogonally polarized fiber modes is removed because of these factors, and the fiber acquires birefringence depending on mode indices for the orthogonally polarized fiber modes .

$$B_m = |\bar{n}_x - \bar{n}_y|,$$

Birefringence leads to a periodic power exchange between the two polarization components. The period, referred to as the beat length:

$$L_B = \lambda / B_m. \qquad \textbf{Dem.}$$

polarization in a birefringent fiber over one beat length. Input beam is linearly polarized at 45◦ with respect to the slow and fast axes.

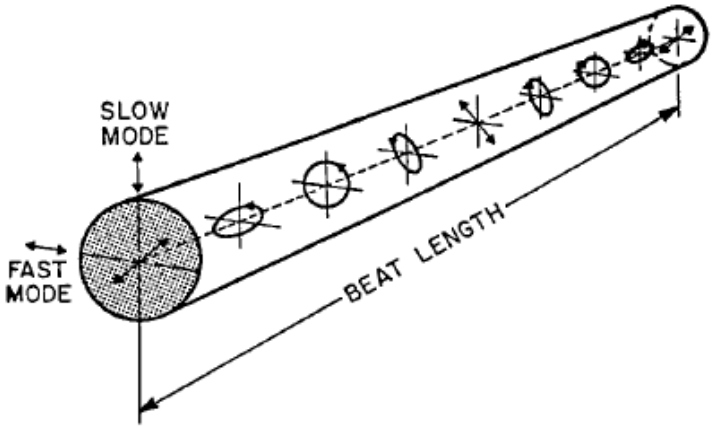

Light launched into the fiber with linear polarization quickly reaches a state of arbitrary polarization. Moreover, different frequency components of a pulse acquire different polarization states, resulting in pulse broadening. This phenomenon is called **polarization-mode dispersion (PMD)** and becomes a limiting factor for optical communication systems operating at high bit rates.

In **PM fibers or polarization-maintaining fibers,** a large amount of birefringence is introduced intentionally through design modifications so that small random birefringence fluctuations do not affect the light polarization significantly. Typically, $B_m \sim 10^{-4}$ for such fibers.

Spot Size

References: Fiber optic Communication System, third Edition, G. P. Agraval - John Wiley & Sons pp 36-47, Lecture notes DEMONSTRATION_2

Electromagnetic field is often approximated by a Gaussian distribution of the form:

$$E_x = A\exp(-\rho^2/w^2)\exp(i\beta z),$$

w is the field radius and is referred to as the spot size, **a is the fiber radius**

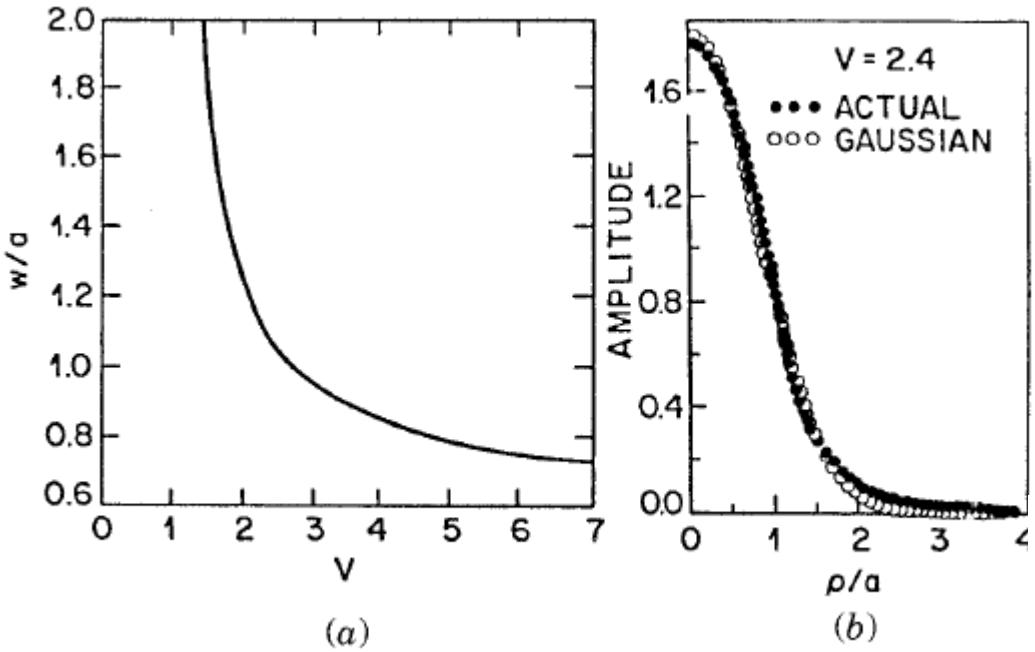

$$V = k_0 a (n_1^2 - n_2^2)^{1/2}$$

The *effective core area*, defined as $A_{eff} = \pi w^2$, is an important parameter for optical fibers as it determines how tightly light is confined to the core.

the *confinement factor:*

$$\Gamma = \frac{P_{core}}{P_{total}} = \frac{\int_0^a |E_x|^2 \rho\, d\rho}{\int_0^\infty |E_x|^2 \rho\, d\rho} = 1 - \exp\left(-\frac{2a^2}{w^2}\right)$$

(a) Normalized spot size *w/a* as a function of the *V* parameter obtained by fitting the fundamental fiber mode to a Gaussian distribution; (b) quality of fit for *V* =2.4.

Most of TLC single-mode fibers are designed to operate in the range 2<V <2.4.

Laser ad itterbio in fibra ottica

i)

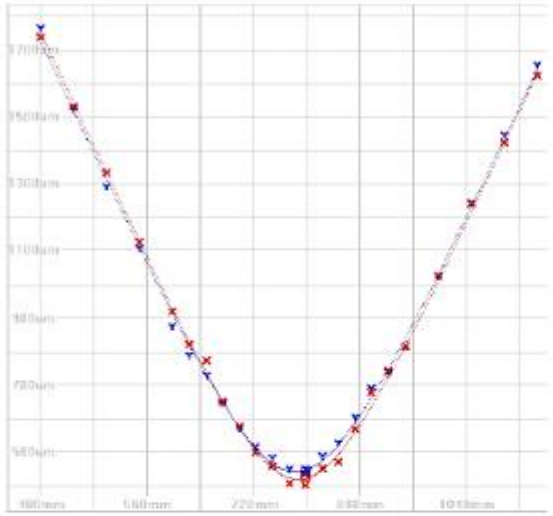

ii)

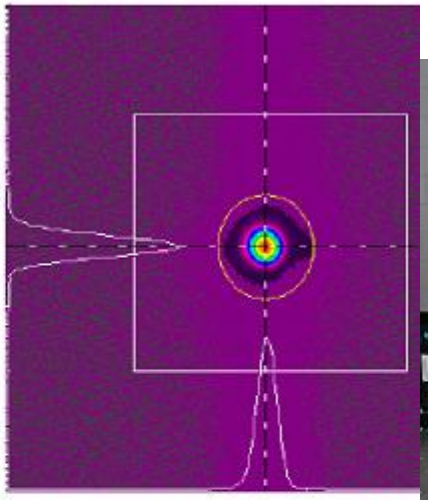

iii)

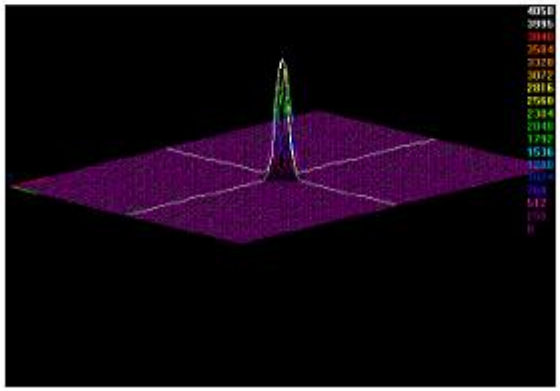

NanoScan PHOTON INC.

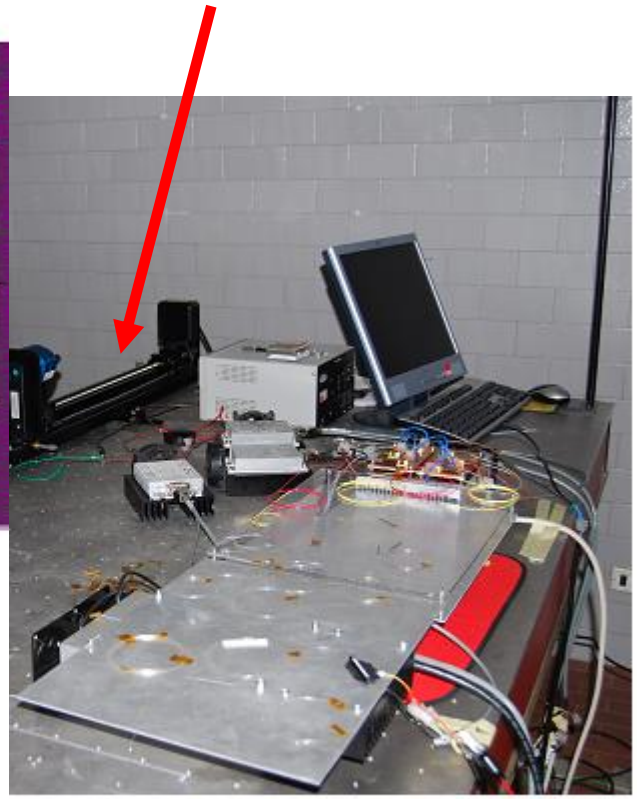

ı M^2 mesaurement system

Elevata qualità di fascio M^2 = 1.33 at 6.2W output power

Laser ad itterbio in fibra ottica

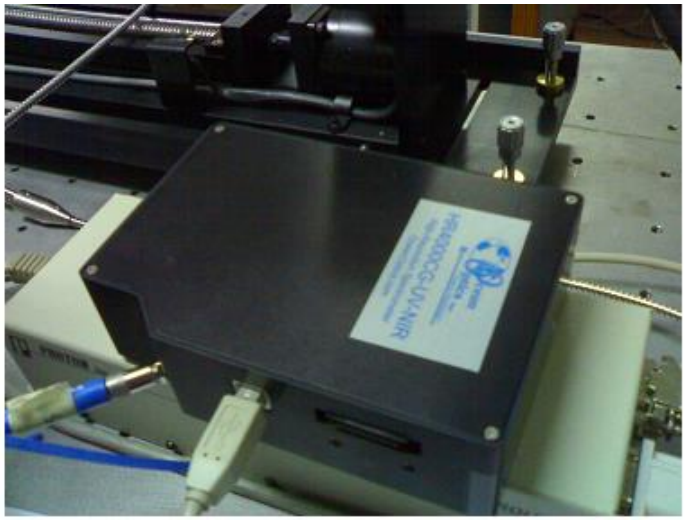

HR4000CG UV-NIR Ocean Optics

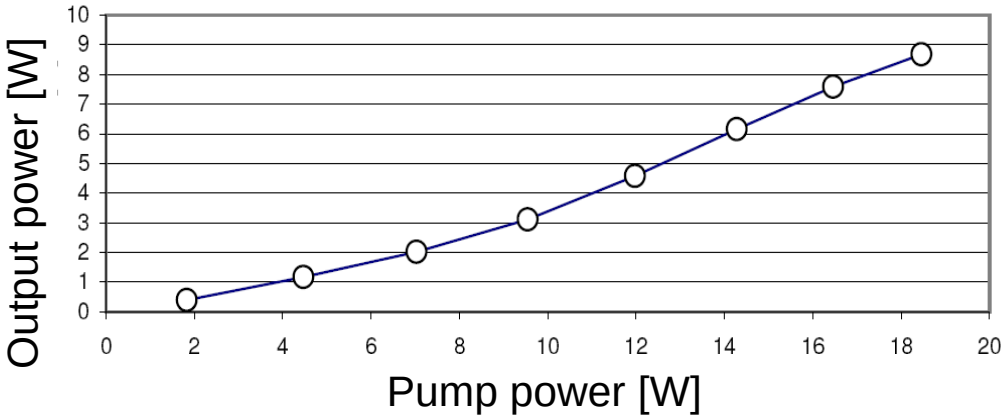

Picco di emissione al variare della lunghezza d'onda stabile grazie al controllo termico

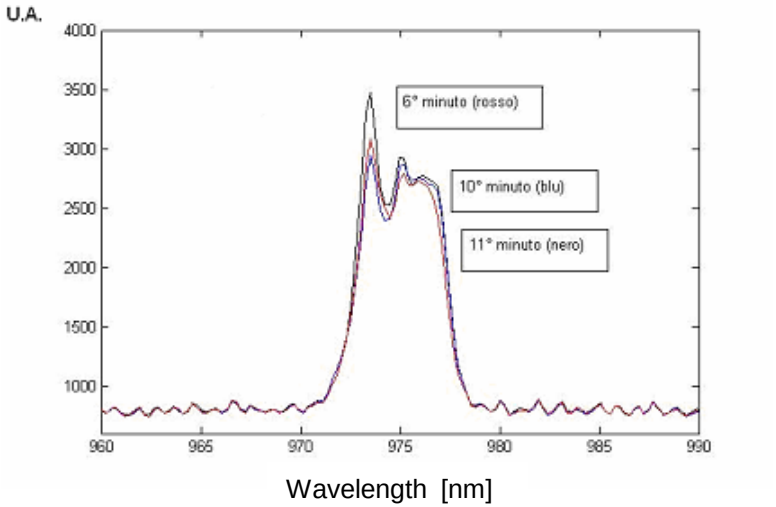

Spettro of laser Bookham laser diode E0014772 per diversi tempi di funzionamento

Dispersion in Single-Mode Fibers

FOR MULTIMODE FIBER in the geometrical-optics description, broadening is attributed to **different paths followed by different rays. In the modal description it is related to the different mode indices (or group velocities) associated with different modes. This is the intermodal dispersion**

The main advantage of **single-mode fibers is that intermodal dispersion is absent** simply because the energy of the injected pulse is transported by a single mode. However, pulse broadening does not disappear altogether.

The group velocity associated with the fundamental mode is frequency dependent because of **chromatic dispersion.** As a result, different spectral components of the pulse travel at slightly different group velocities, a phenomenon referred to as:

Group-Velocity Dispersion (GVD), intramodal dispersion, or simply fiber dispersion.

Intramodal dispersion has two contributions:

material dispersion and waveguide dispersion.

$$n^2(\omega) = 1 + \sum_{j=1}^{M} \frac{B_j \omega_j^2}{\omega_j^2 - \omega^2},$$

$$V = k_0 a (n_1^2 - n_2^2)^{1/2}$$

Group-Velocity Dispersion

Consider a single-mode fiber of length *L*. **A specific spectral component at the frequency ω would arrive at the output end of the fiber after a time delay *T* = *L*/*v*$_g$, where *v*$_g$ is the *group velocity***, defined as

$$v_g = (d\beta/d\omega)^{-1}.$$

$$\beta = \bar{n}k_0 = \bar{n}\omega/c$$

$$v_g = c/\bar{n}_g, \qquad \bar{n}_g = \bar{n} + \omega(d\bar{n}/d\omega). \qquad \textbf{Dem.}$$

Δω is the spectral width of the pulse,

$$\Delta T = \frac{dT}{d\omega}\Delta\omega = \frac{d}{d\omega}\left(\frac{L}{v_g}\right)\Delta\omega = L\frac{d^2\beta}{d\omega^2}\Delta\omega = L\beta_2\Delta\omega, \qquad \textbf{Dem.}$$

$\beta_2 = d^2\beta/d\omega^2$ is known as the **GVD parameter.**

It is customary to use Δλ in place of Δω.

$$\omega = 2\pi c/\lambda$$

$$\Delta\omega = (-2\pi c/\lambda^2)\Delta\lambda$$

$$v_g = (d\beta/d\omega)^{-1}.$$

$$\Delta T = \frac{d}{d\lambda}\left(\frac{L}{v_g}\right)\Delta\lambda = DL\Delta\lambda,$$

Dem.

$$D = \frac{d}{d\lambda}\left(\frac{1}{v_g}\right) = -\frac{2\pi c}{\lambda^2}\beta_2.$$

D is called the **dispersion parameter** and is expressed in units of ps/(km-nm).

The effect of dispersion on the bit rate B can be estimated by using the criterion $B\Delta T < 1 \qquad BL|D|\Delta\lambda < 1.$ **Dem.**

$$V = k_0 a (n_1^2 - n_2^2)^{1/2}$$

$$D = \frac{d}{d\lambda}\left(\frac{1}{v_g}\right) = -\frac{2\pi c}{\lambda^2}\beta_2.$$

$$D = -\frac{2\pi c}{\lambda^2}\frac{d}{d\omega}\left(\frac{1}{v_g}\right) = -\frac{2\pi}{\lambda^2}\left(2\frac{d\bar{n}}{d\omega} + \omega\frac{d^2\bar{n}}{d\omega^2}\right).$$ **Dem.**

Moreover, *D* can be written as the sum of two terms, $D = D_M + D_W,$

the material dispersion D_M and the waveguide dispersion D_W

$$D_M = -\frac{2\pi}{\lambda^2}\frac{dn_{2g}}{d\omega} = \frac{1}{c}\frac{dn_{2g}}{d\lambda},$$

$$b = \frac{\beta/k_0 - n_2}{n_1 - n_2} = \frac{\bar{n} - n_2}{n_1 - n_2}.$$

$$D_W = -\frac{2\pi\Delta}{\lambda^2}\left[\frac{n_{2g}^2}{n_2\omega}\frac{Vd^2(Vb)}{dV^2} + \frac{dn_{2g}}{d\omega}\frac{d(Vb)}{dV}\right]$$

$$\bar{n} = n_2 + b(n_1 - n_2) \approx n_2(1 + b\Delta)$$ **Dem.**

Here n_{2g} is the group index of the cladding material **Dem.**

$$BL|D|\Delta\lambda < 1.$$

D is relatively small **in the wavelength region near 1.3 μm [D ~ 1 ps/(km-nm)].** For a semiconductor laser, the spectral width **Δλ is 2–4 nm** even when the laser operates in several longitudinal modes. The BL product of such lightwave systems can exceed **100 (Gb/s)-km**. Indeed, 1.3-μm telecommunication systems typically operate at a bit rate of **2 Gb/s with a repeater spacing of 40–50 km.** The BL product of single-mode fibers can exceed 1 (Tb/s)-km when singlemode semiconductor lasers are used to reduce Δλ below 1 nm.

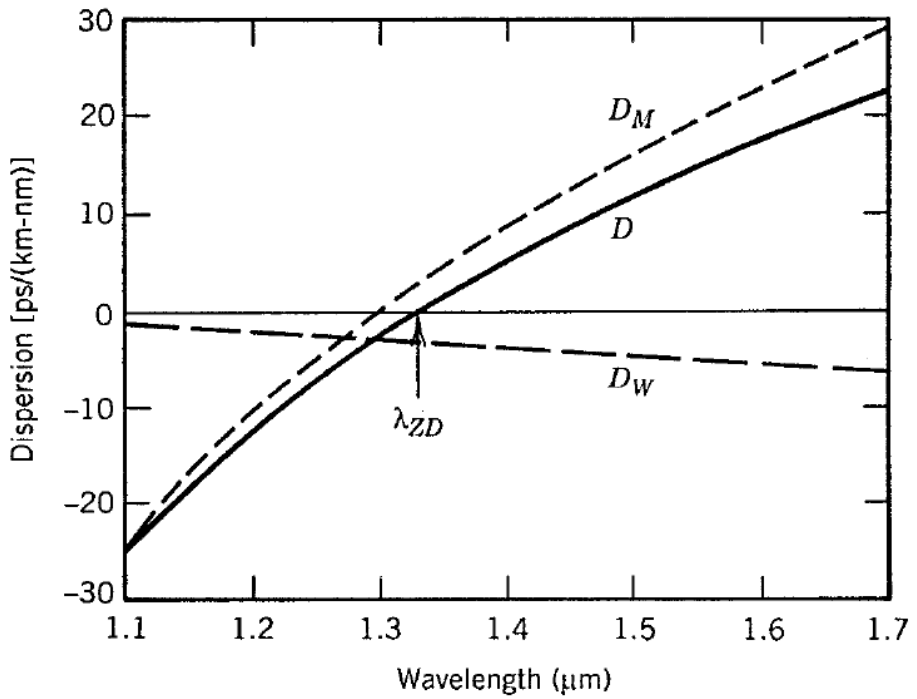

For an example of GVD and D control /refractiver index tailoring optionally see the paper: A. DI TOMMASO, M. DE SARIO, L. MESCIA, F. PRUDENZANO: "Numerical analysis of aperiodic photonic crystal fiber for supercontinuum generation" Optical Engineering 51 (3), 035003 (March 2012) pp 035003-1 35003-7- DOI: 10.1117/1.OE.51.3.035003 ISSN: 0091-3286

$$D = D_M + D_W,$$

The main effect of waveguide dispersion is to shift λ_{ZD} by an amount 30–40 nm so that the total dispersion is zero near 1.31 μm.

Total dispersion *D* and relative contributions of material dispersion D_M and waveguide dispersion D_W for a conventional single-mode fiber. The zero-dispersion wavelength shifts to a higher value because of the waveguide contribution

Since the waveguide contribution D_W depends on fiber parameters such as the core radius *a* and the index difference Δ, it is possible to design the fiber such that λ_{ZD} is shifted into the vicinity of 1.55 μm (where the minimum of losses occurs)

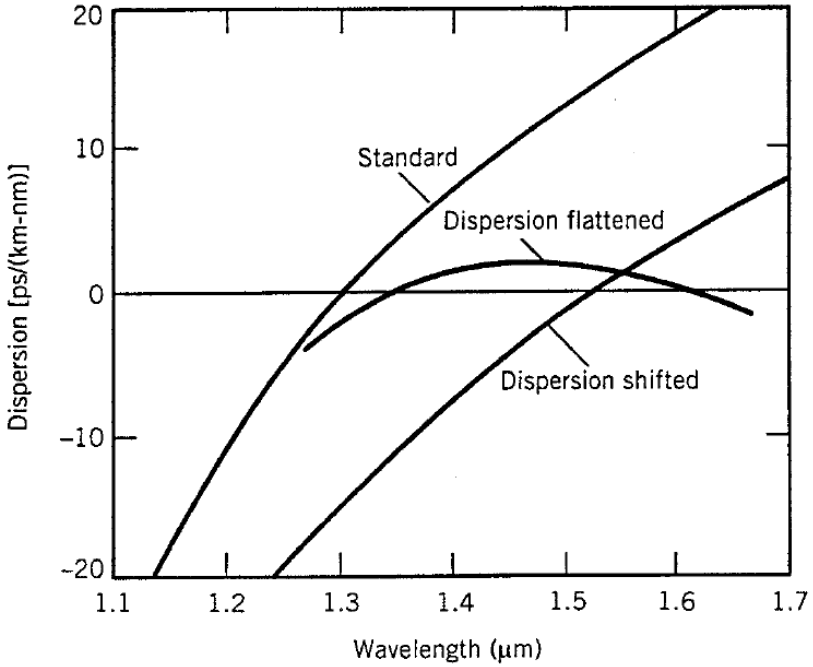

$$BL|D|\Delta\lambda < 1.$$

DW depends on fiber parameters such as the core radius *a* and the index difference Δ, it is possible to design the fiber such that λ_{ZD} is shifted into the vicinity of 1.55 μm. Such fibers are called ***dispersion shifted*** fibers. It is also possible to tailor the waveguide contribution such that the total dispersion *D* is relatively small over a wide wavelength range extending from 1.3 to 1.6 μm. Such fibers are called ***dispersion-flattened*** fibers.

The BL product of a single-mode fiber can be increased by operating at the zero-dispersion wavelength λ_{ZD} where D = 0.

Higher-Order Dispersion

$$BL|D|\Delta\lambda < 1.$$

$$B\Delta T < 1$$

It appears that the *BL* product of a single-mode fiber can be increased indefinitely by operating at the zero-dispersion wavelength λ_{ZD} where $D = 0$. **The dispersive effects, however, do not disappear completely at $\lambda = \lambda_{ZD}$.**

S dispersion slope

$$S = dD/d\lambda.$$

S is also called a **differential-dispersion parameter.**

$$D = \frac{d}{d\lambda}\left(\frac{1}{v_g}\right) = -\frac{2\pi c}{\lambda^2}\beta_2.$$

$$S = (2\pi c/\lambda^2)^2\beta_3 + (4\pi c/\lambda^3)\beta_2,$$ **Dem.**

$$\beta_3 = d\beta_2/d\omega \equiv d^3\beta/d\omega^3$$

where $\beta_3 = d\beta_2/d\omega \equiv d^3\beta/d\omega^3$ is the third-order dispersion parameter.

for $\lambda = \lambda_{ZD}$, $\beta_2 = 0$, and ***S* is proportional to β_3.**

We can estimate the limiting bit rate by noting that for a source of spectral width $\Delta\lambda$, the effective value of dispersion parameter becomes ***D* = *S*Δλ**. The limiting bit rate–distance product can now be obtained with this value of *D*. The resulting condition becomes

$$BL|S|(\Delta\lambda)^2 < 1.$$

For a multimode semiconductor laser with Δλ = 2 nm and a dispersion-shifted fiber with S = 0.05 ps/(km-nm^2) at λ = 1.55 μm, the BL product approaches 5 (Tb/s)-km.

Material Absorption

Intrinsic absorption losses correspond to absorption by fused silica (**material used to make fibers**)

Extrinsic absorption is related to losses caused by impurities within silica.

Any material absorbs at certain wavelengths corresponding to the electronic and vibrational resonances associated with specific molecules.

For silica (SiO_2) molecules, **electronic resonances** occur in the **ultraviolet region ($\lambda < 0.4$ μm)**, whereas **vibrational resonances** occur in **the infrared region ($\lambda > 7$ μm).**

Extrinsic absorption results from the presence of impurities. Transition-metal impurities such as **Fe, Cu, Co, Ni, Mn**, and **Cr absorb strongly in the wavelength range 0.6–1.6μm.**

Such high-purity silica can be obtained by using modern techniques. The main source of extrinsic absorption in state-of-the-art silica fibers is thet presence of water vapors.

A vibrational resonance of the **OH ion occurs near 2.73 μm**. **Its harmonic and combination tones with silica produce absorption at the 1.39-, 1.24-, and 0.95-μm wavelengths.**

The three spectral peaks seen in occur near these wavelengths and are due to the **presence of residual water vapor in silica.** Even a concentration of **1 part per million can cause a loss of about 50 dB/km at 1.39 μm.**

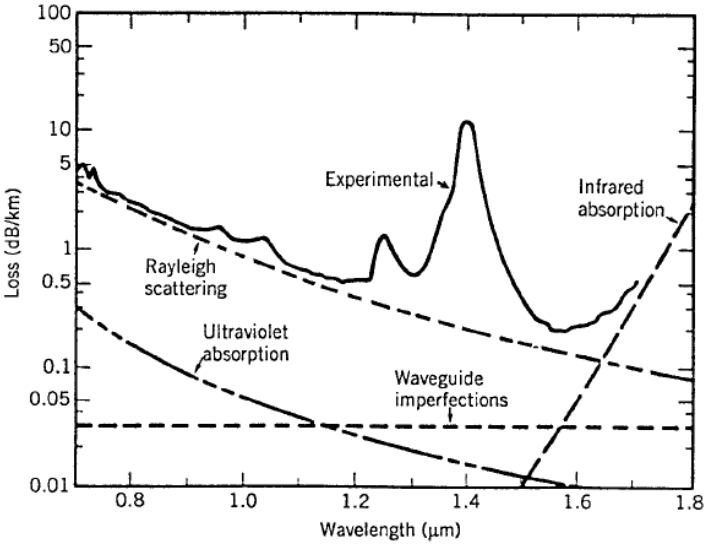

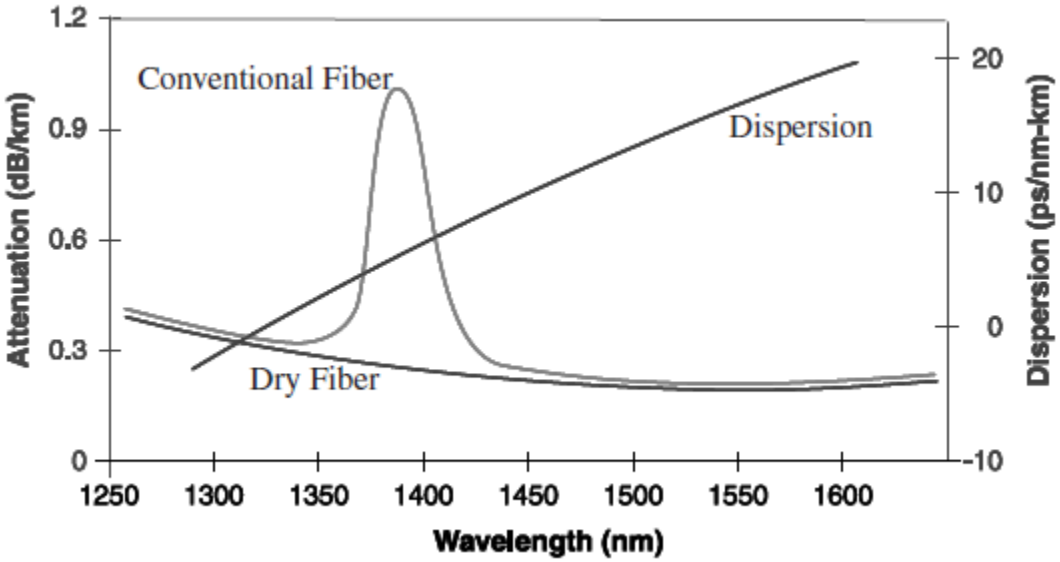

The **OH ion concentration is reduced to below 10^{-8} in modern fibers** to lower **the 1.39-μm peak below 1 dB.** In a new kind of fiber, known as the ***dry fiber***, the OH ion concentration is reduced to such low levels that the 1.39-μm peak almost disappears

Silica fibers cannot be used in the wavelength region beyond 2 μm, since infrared absorption begins to dominate the fiber loss beyond 1.6 μm. Considerable effort has been directed toward finding other suitable materials with low absorption beyond 2 μm

Fluorozirconate (ZrF 4) fibers have an intrinsic material absorption of about 0.01 dB/km **near 2.55 μm** and have the potential for exhibiting loss much smaller than that of silica fibers. State-of-the-art **fluoride fibers, however, exhibit a loss of about 1 dB/km** because of extrinsic losses.

Chalcogenide and polycrystalline fibers exhibit minimum loss in the far-infrared region near 10 μm. The theoretically predicted minimum value of fiber **loss for such fibers is below 10^{-3} dB/km because of reduced Rayleigh scattering.**

Tellurite glass fiber are a good alternative to chalcogenide ones

Microstructured Fibers

Microstructured optical fibers

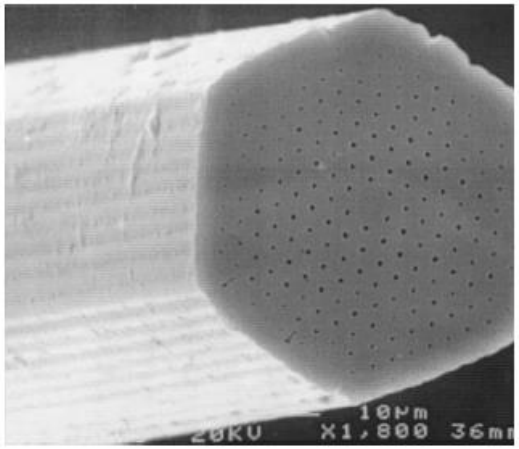

J.C. Knight, T. A. Birks, P. St. J. Russel, D. M. Aktin, "All silica single mode optical fiber with photoniccrystal cladding," Opt. Lett., vol. 21, pp. 1547-1549, 1996.

Air holes

- Short fiber length
- Improvement of pump absorption
- Minimization of length-dependent nonlinear effects
- Residual pump power reduction

Large controllable refractive index variation

Core design flexibility

High precision in handling the core and cladding refractive indices….Approximately 10^{-5}

Large, ultralow numerical aperture, single-mode core

Very high numerical aperture for the pump core

High overlap between pump light and active ions in the signal core
Higher pump absorption and shorter fiber length

Active air-clad fibers

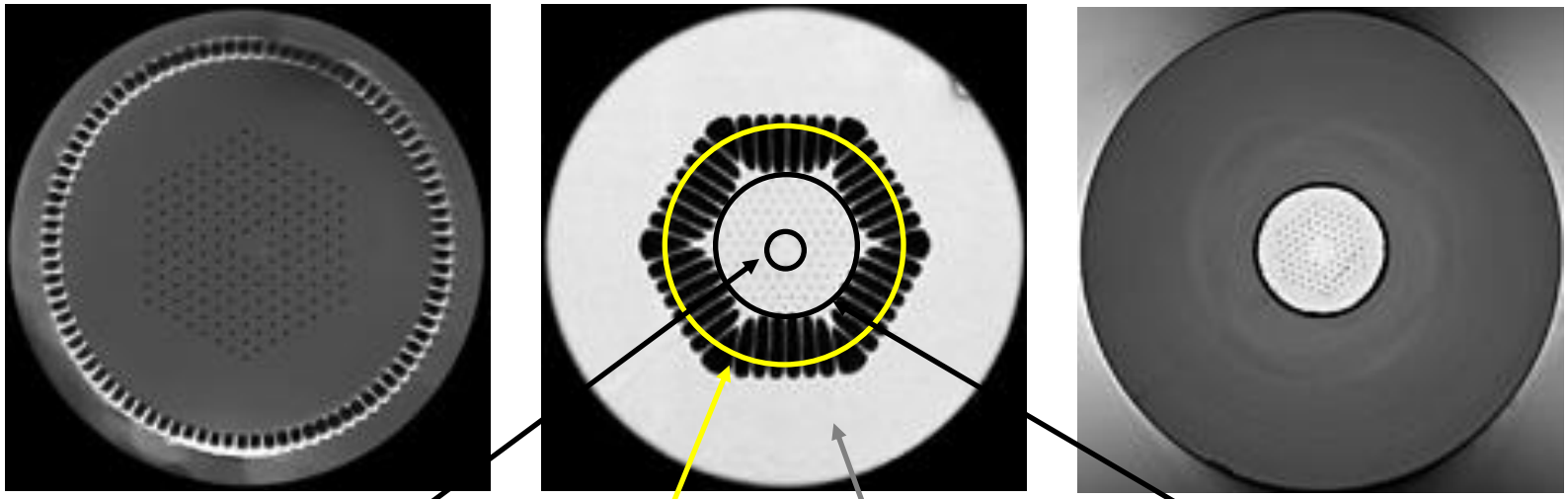

www.blazephotonics.com

Active core

Air-silica microstrutured inner cladding

Ring of large air-holes

Solid silica overcladding

Stimulated Brillouin Scattering AMPLIFIERS/LASERS

The physical process behind Brillouin scattering is the tendency of materials to become compressed in the presence of an electric field a phenomenon termed **electrostriction**

For an oscillating electric field at the pump frequency Ω_p, this process **generates an acoustic wave at some frequency Ω.**

Spontaneous Brillouin scattering can be viewed as scattering of the pump wave from this acoustic wave, resulting in creation of a new wave at the frequency Ω_s. The scattering process must conserve both the **energy** and the **momentum**.

The energy conservation requires that the **Stokes shift** $\Omega = \Omega_A$ equals $\omega_p - \omega_s$. **The momentum conservation requires** that the **wave vectors** satisfy $\mathbf{k}_A = \mathbf{k}_p - \mathbf{k}_s$.

Using the dispersion relation $|\boldsymbol{k}_A| = \Omega/\boldsymbol{v}_A$, where $\boldsymbol{v}_A$ **is the acoustic velocity**, this condition determines the acoustic frequency as

$$\Omega = |k_A| v_A = 2 v_A |k_p| \sin(\theta/2), \qquad \textbf{DIM}$$

where $|\mathbf{k}_p| \approx |\mathbf{k}_s|$ was used and **θ represents the angle between the pump and scattered waves**. Note that **Ω vanishes in the forward direction** (θ = 0) and **is maximum in the backward direction (θ =π).**

The SBS gain g_B is frequency dependent because of a **finite damping time T_B of acoustic waves** (**the lifetime of acoustic phonons**). If the acoustic waves decay as $\exp(-t/T_B)$, the Brillouin gain has a Lorentzian spectral profile given by

$$g_B(\Omega) = \frac{g_B(\Omega_B)}{1 + (\Omega - \Omega_B)^2 T_B^2}.$$

The **threshold power level for STIMULATED BRILLUIN SCATTERING SBS can be estimated by solving the previous differential Eqs. and finding at what value of I_p, I_s grows from noise to a significant level.** The threshold power $P_{th} = I_p A_{eff}$, where A_{eff} is the effective core area, satisfies the condition

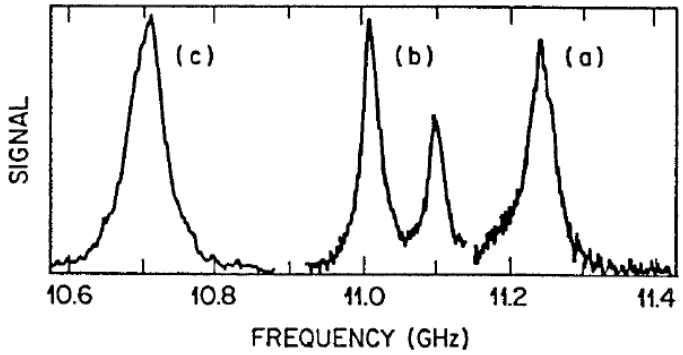

Figure 2.17: Brillouin-gain spectra measured using a 1.525-μm pump for three fibers with different germania doping: (a) silica-core fiber; (b) depressed-cladding fiber; (c) dispersion-shifted fiber. Vertical scale is arbitrary. (After Ref. [78]; ©1986 IEE; reprinted with permission.)

$$g_B P_{th} L_{eff} / A_{eff} \approx 21,$$
$$L_{eff} = [1 - \exp(-\alpha L)]/\alpha.$$

The threshold power P_{th} is defined as the incident power at which half of the pump power is transferred to the Stokes field at the output end of a fiber of length L.

α represents fiber losses. For optical communication systems L_{eff} can be approximated by 1/α as $\alpha L >> 1$. Using $A_{eff} = \pi w^2$, where w is the spot size, P_{th} can be as low as 1 mW depending on the values of w and α

Stimulated Raman Scattering AMPLIFIERS/LASERS

Spontaneous Raman scattering occurs in optical fibers when a pump wave is scattered by the silica molecules.

Source that derives molecular oscillations.

vibrational energy levels of silica dictate the value of the Raman shift $\Omega_R = \omega_p - \omega_s$.

As an acoustic wave is not involved, spontaneous Raman scattering is an isotropic process and occurs in all directions.

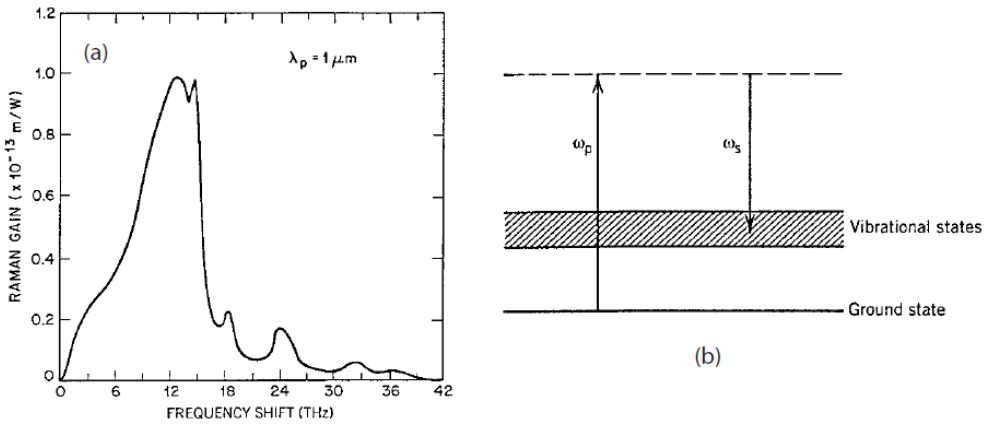

Figure 2.18: (a) Raman gain spectrum of fused silica at $\lambda_p = 1\,\mu$m and (b) energy levels participating in the SRS process. (After Ref. [75]; ©1972 AIP; reprinted with permission.)

Similar to the SBS case, the Raman scattering process becomes **STIMULATED RAMAN SCATTERING** if the **pump power exceeds a threshold value. SRS can occur in both the forward and backward directions** in optical fibers.

Physically speaking, the beating of the pump and with the scattered light in these two directions creates a frequency component at the beat frequency $\omega_p - \omega_s$, which acts as a source that derives molecular oscillations.

Since the amplitude of the scattered wave increases in response to these oscillations, a positive feedback loop sets in.

Supercontinuum (SC) generation

Supercontinuum (SC) generation refers to the nonlinear phenomenon occurring when narrow-band incident light pulses are affected by a plethora of nonlinear effects yielding a broadband beam.

In optical fibers, it involves purely temporal dynamics processes. Optical fibers allow longer interaction lengths and higher effective nonlinearities, leading to significant reductions of the pulse peak power.

In the **normal dispersion regime (negative dispersion), Raman scattering and self-phase modulation (SPM) are the main effects** that induce spectral broadening. In the anomalous dispersion regime (positive dispersion), **the interaction between soliton fission, Raman self-frequency shift, and dispersive waves allows SC generation**.

Spectral broadening, obtained by means of novel kinds of PCF fibers, promises innovative applications. As an example, the SC sources are employed for tunable ultrafast **femtosecond generation**, dense wavelength division multiplexing (DWDM), and for ultra-high-resolution optical **coherence tomography** in **morphological imaging of biological tissue on a micrometer scale**. In particular, SC generation via fs pulses allows a spectral broadening

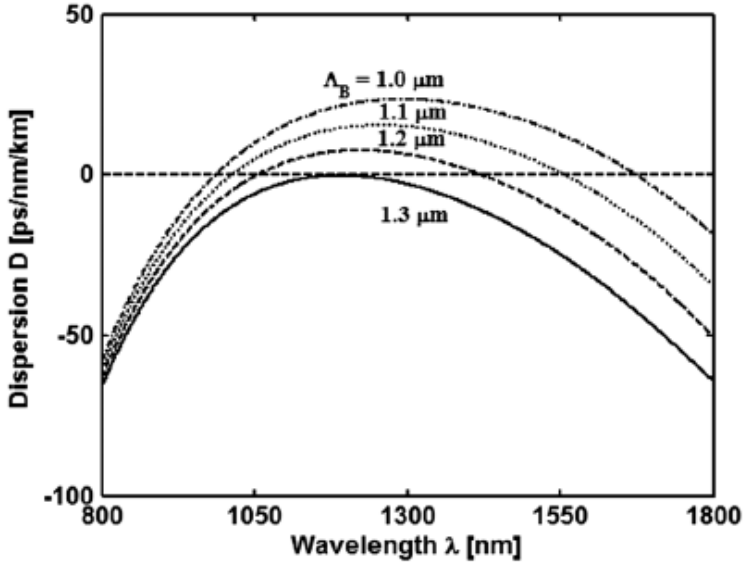

Fig. 3 Dispersion curves for $ThMoT_3$ PCF with hole diameter $D_h = 0.5\ \mu m$, first pitch $\Lambda_A = 1.7\ \mu m$, second pitch $\Lambda_B = 1.0,\ 1.1,\ 1.2,\ 1.3\ \mu m$.

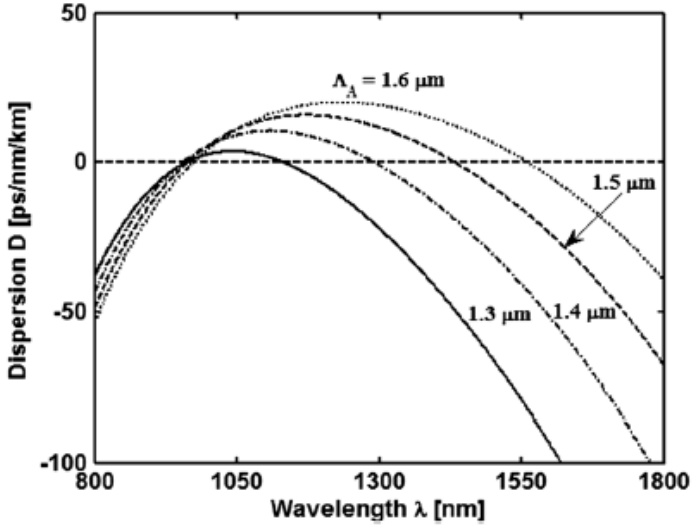

Fig. 4 Dispersion curves for $ThMoT_3$ PCF with hole diameter $D_h = 0.5\ \mu m$, first pitch $\Lambda_A = 1.3,\ 1.4,\ 1.5,\ 1.6\ \mu m$, second pitch $\Lambda_B = 1.0\ \mu m$.

For each ThMoT3 dispersion curve of Figs. 3, 4, and 5, **the corresponding higher-order dispersion coefficients are calculated.** Moreover, the effective mode areas of theinvestigated ThMoT3 PCFs are calculated. As expected, the effective mode area increases by increasing the wavelength. This phenomenon is mainly due to the reduced bounding of the mode electromagnetic field at longer wavelengths.

Optical Engineering

SPIEDigitalLibrary.org/oe

Numerical analysis of aperiodic photonic crystal fiber structures for supercontinuum generation

Annalisa Di Tommaso
Marco De Sario
Luciano Mescia
Francesco Prudenzano

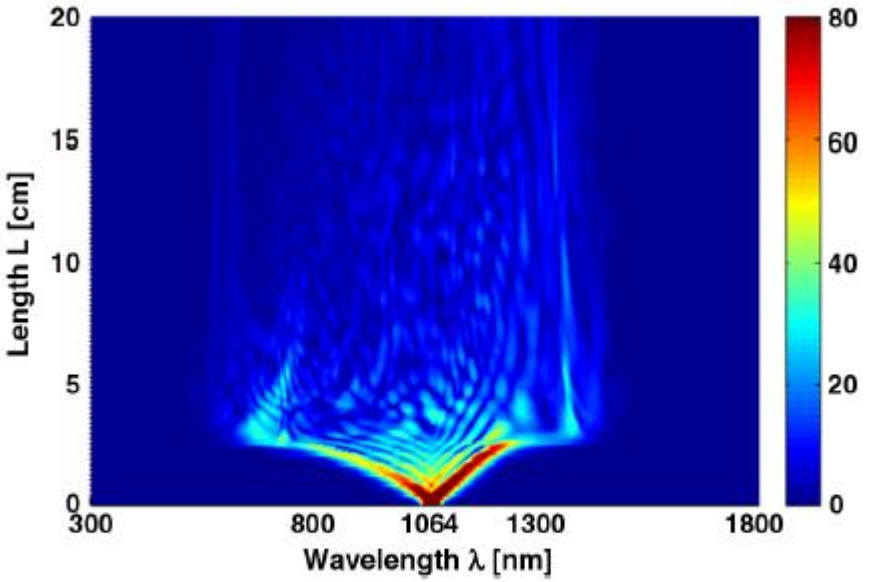

ig. 10 Spectral evolution density plot for the $ThMoT_3$ PCF ith $D_h = 0.5\ \mu m$, $\Lambda_A = 1.4\ \mu m$, $\Lambda_B = 1.0\ \mu m$, input pulse with WHM = 100 fs, peak power 15 kW.

MICROSTRUCTURED FIBER FOR: **SUPERCONTINUUM GENERATION**, **SOLITON PROPAGATION, DISPERSION COMPENSATION**

Fiber Solitons

The existence of solitons in optical fibers is the result of a **balance between the group velocity dispersion (GVD) and self-phase modulation (SPM),** Tthe GVD broadens optical pulses during their propagation inside an optical fiber except when the pulse is initially chirped in the right way. More specifically, a chirped pulse can be compressed during the early stage of propagation whenever the GVD parameter β_2

Basic NLS propagation equation that governs pulse evolution inside a single-mode fiber

$$\frac{\partial A}{\partial z}+\beta_1\frac{\partial A}{\partial t}+\frac{i\beta_2}{2}\frac{\partial^2 A}{\partial t^2}-\frac{\beta_3}{6}\frac{\partial^3 A}{\partial t^3}=0.$$

$\beta_1 = 1/v_g$, where v_g is the group velocity. The GVD coefficient β_2 is related to the dispersion parameter *D*, whereas β_3 is related to the dispersion slope *S*.

Self-Phase Modulation

$$\beta' = \beta + k_0\bar{n}_2 P/A_{\text{eff}} \equiv \beta + \gamma P,$$

$$\gamma = 2\pi\bar{n}_2/(A_{\text{eff}}\lambda)$$

If we use first-order perturbation theory to see how fiber modes are affected by the nonlinear term, we find that the **mode shape does not change** but the propagation constant becomes power dependent. It can be written as

The amplitude derivative with respect to z is $i\gamma|A|^2A$

The amplitude derivative with respect to z is $-\frac{\alpha}{2}A,$

Design of an Efficient Pumping Scheme for Mid-IR Dy^{3+}:$Ga_5Ge_{20}Sb_{10}S_{65}$ PCF Fiber Laser

Mario Christian Falconi, *Student Member, IEEE*, Giuseppe Palma, Florent Starecki, Virginie Nazabal, Johann Troles, Stefano Taccheo, Maurizio Ferrari, and Francesco Prudenzano

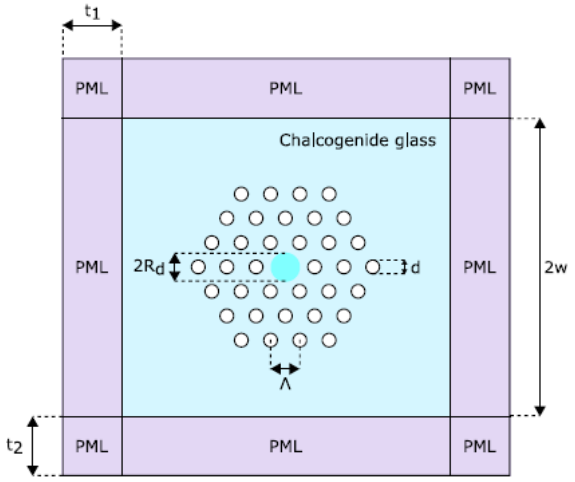

Fig. 1. Cross-section of the photonic crystal fiber.

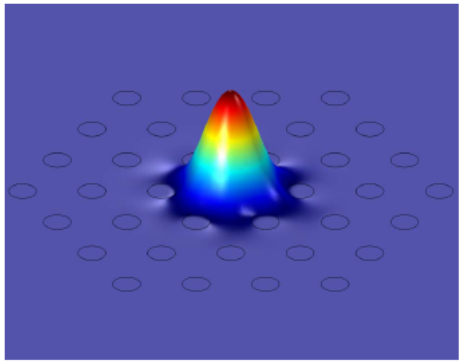

Fig. 2. Distribution of the electric field norm for the fundamental mode at signal wavelength $\lambda_s = 4384$ nm.

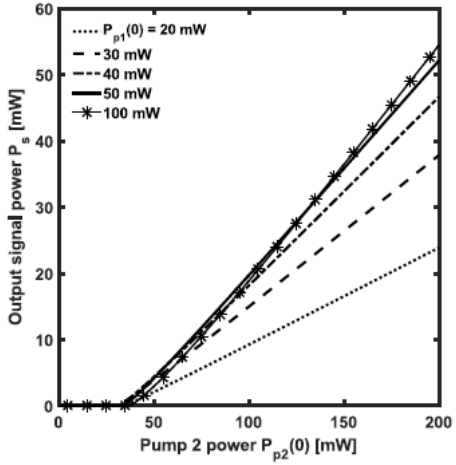

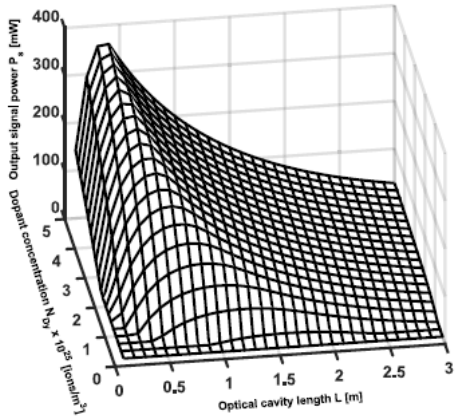

amplifier ansd lasers

265

cillator

ssion

l, Johann Troles,

agram of

in

dition

$$\frac{1}{\sqrt{R_1 R_2}}$$

Development of a 15 W CW Yb doped glass laser

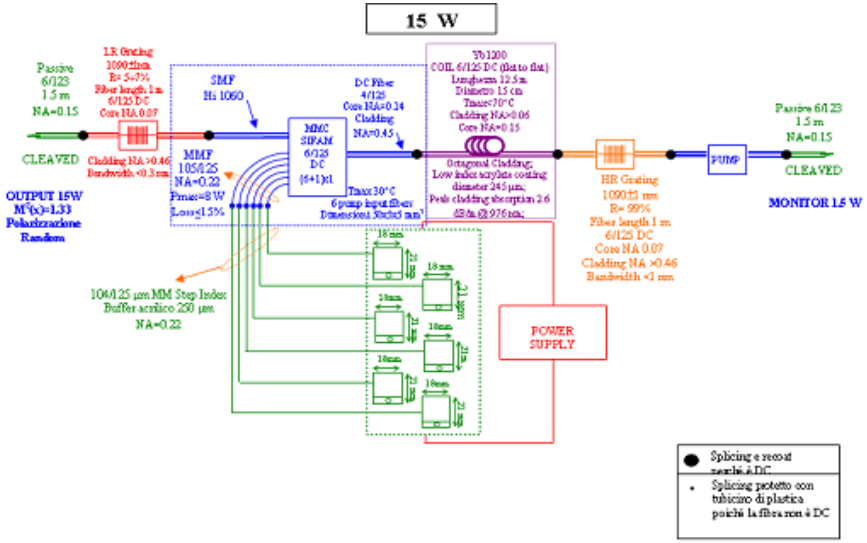

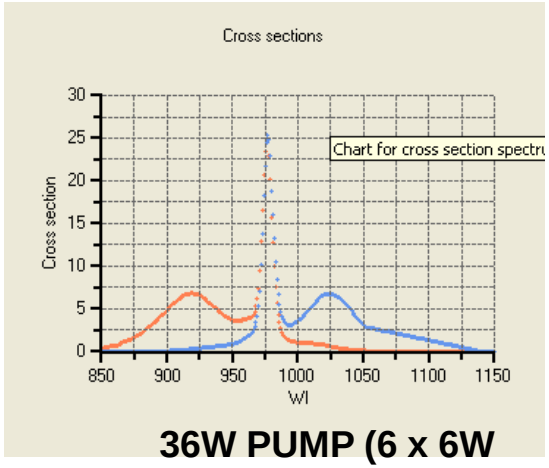

36W PUMP (6 x 6W PUMP DIODES)

15 W CW Yb doped fiber laser

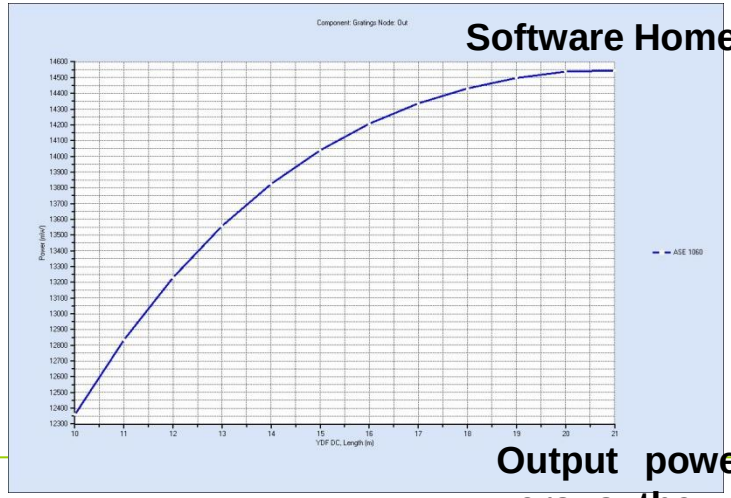

Software Home-made

L_{opt}= 20 m
P_{out}=14.5 W

Output power at wavelength λ=1080 nm versus the Yb1200-6/125DC fiber length; pump at wavelength 920 nm (home made software)

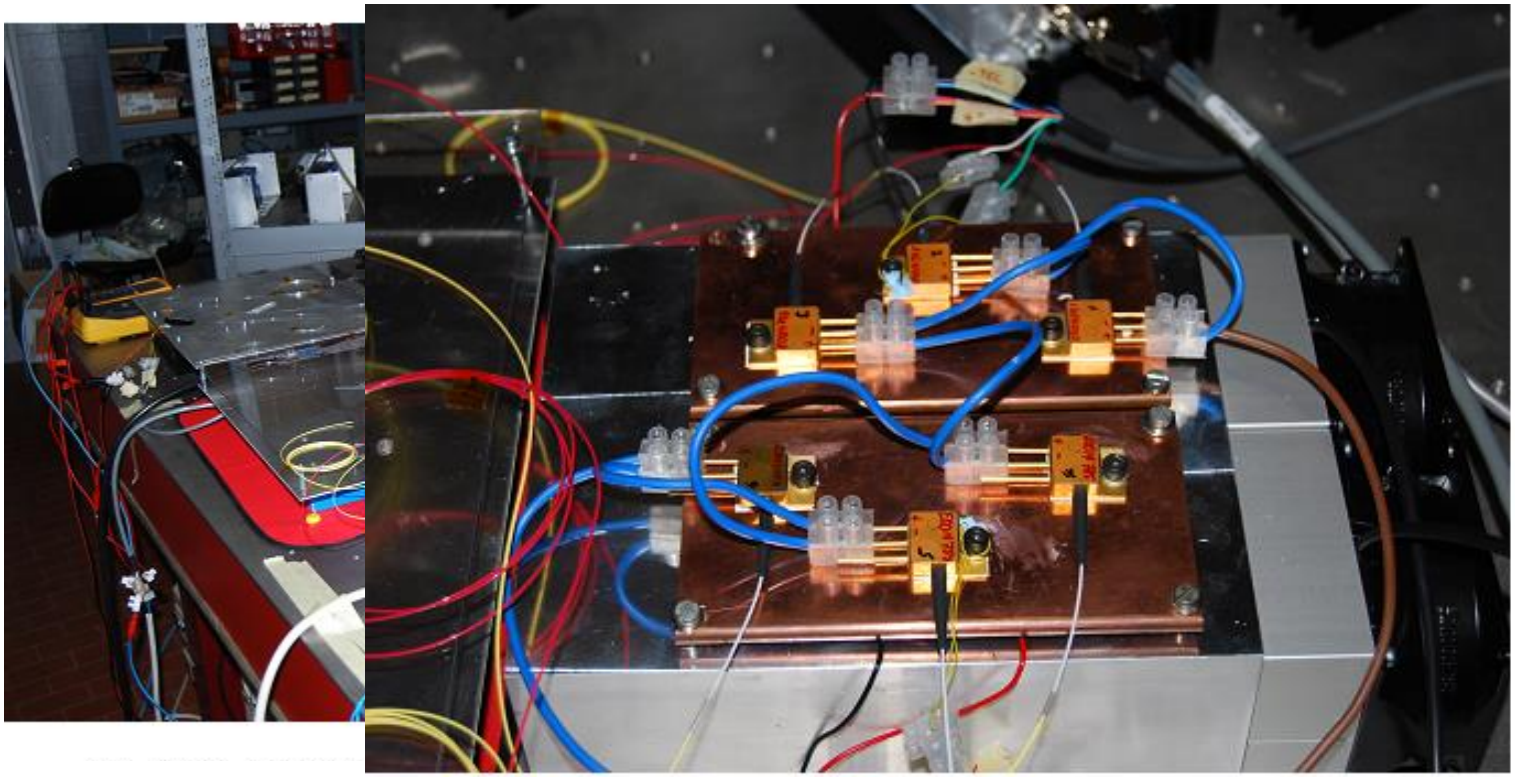

CW 15W Y

Cooling system of the CW 15W Yb doped fiber laser system

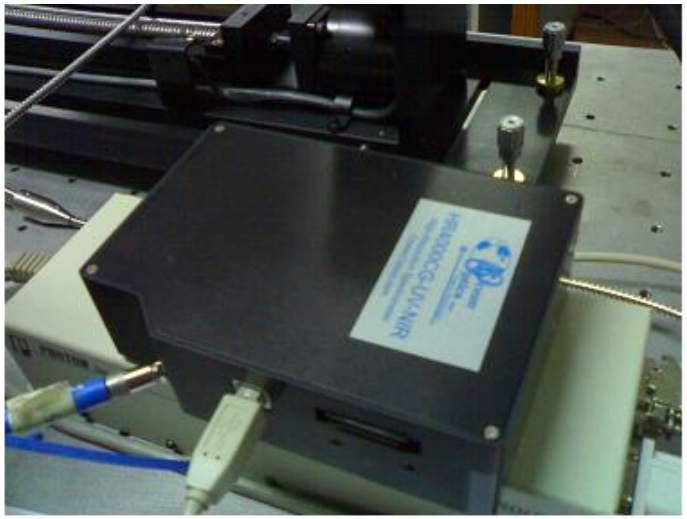

HR4000CG UV-NIR Ocean Optics

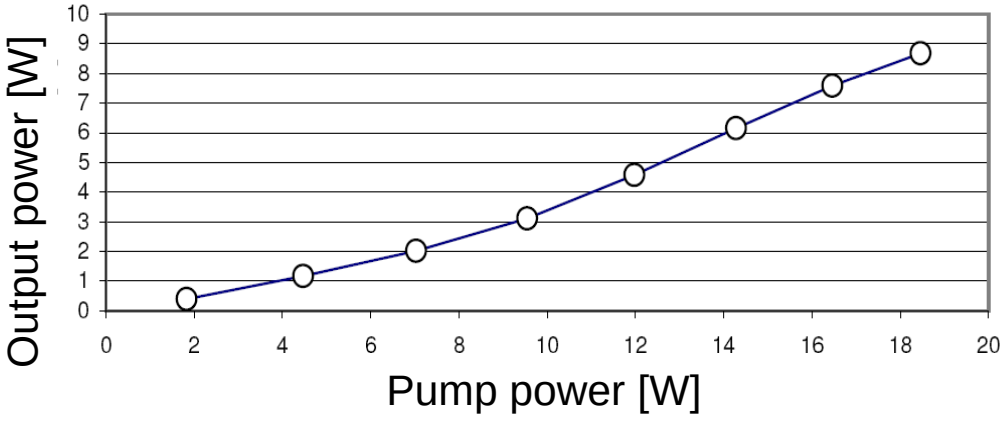

The emission peak versus wavelength and for different operation time is stable because

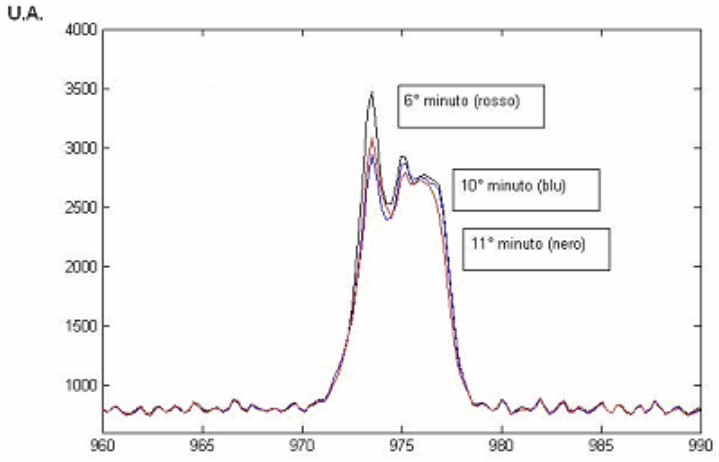

Spectrum of the cooled Bookham laser diode E0014772 for different operating time

i)

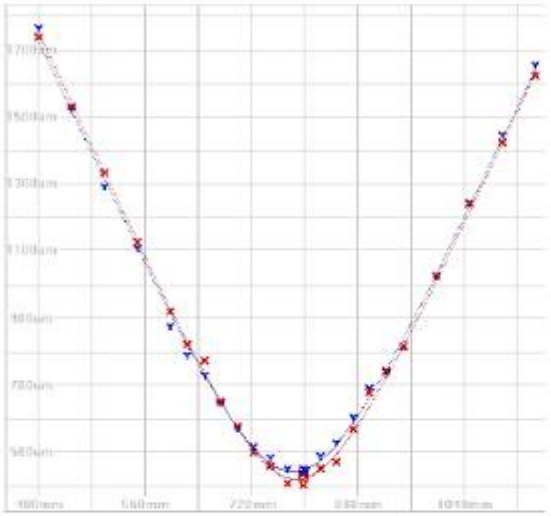

ii)

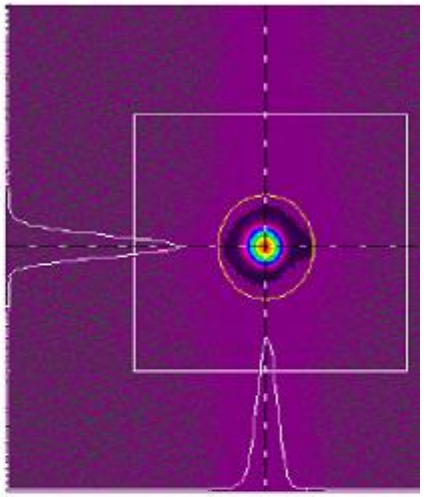

iii)

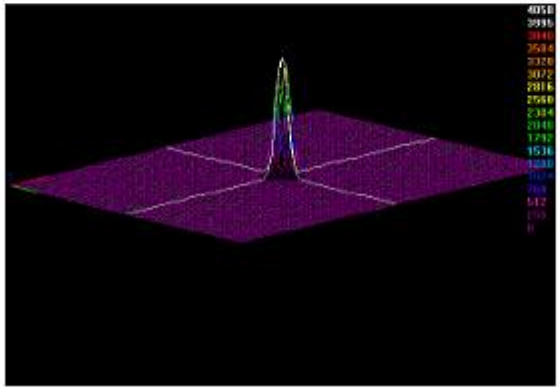

M^2 = 1.33 at 6.2W output power

Development of a 100 W CW Yb doped glass laser

Yb1200 20/400DC

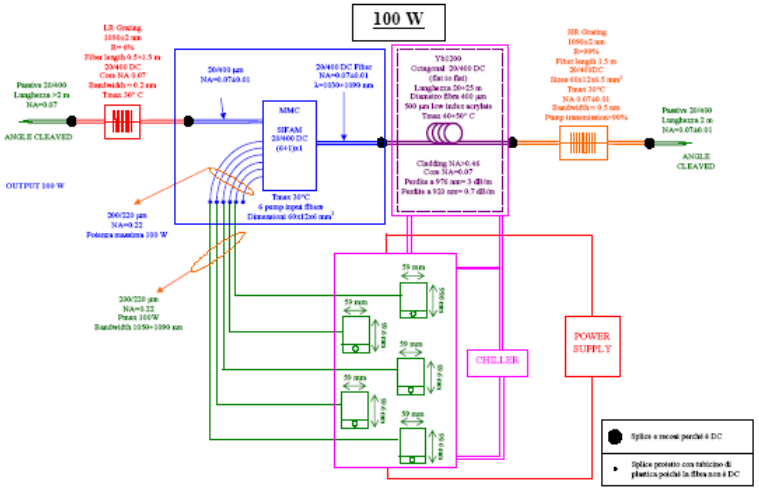

L_{opt}= 21 m Software home made
P_{out}=92 W

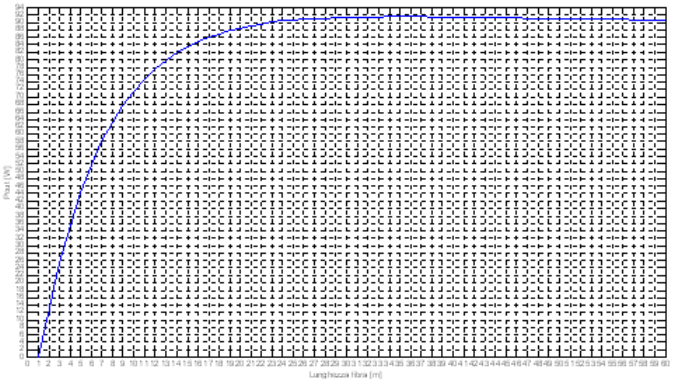

Laser power versus fiber length

CW 100 W Yb doped fiber LASER

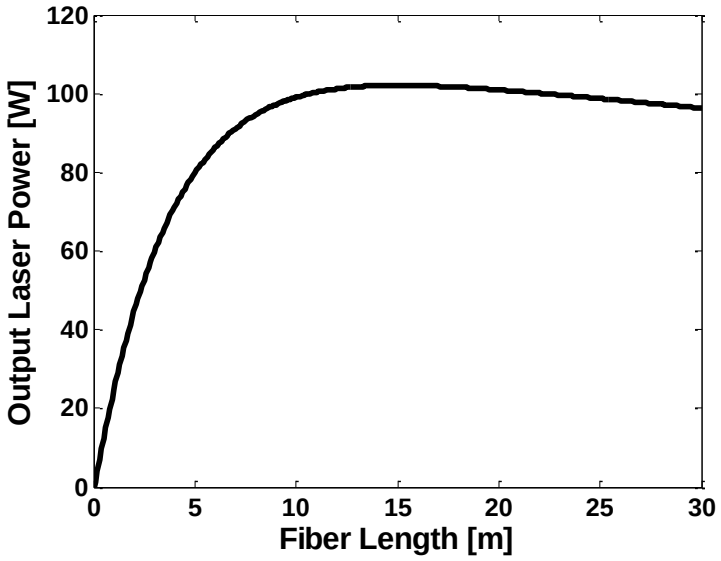

Propagation loss at pump = 0.4 dB/m
Propagation loss at signal = 0.02 dB/m
0.1 dB x 5 splices

100W LASER PUMP at 920 nm
Yb1200 20/400DC
R1= 99%
R2= 6%

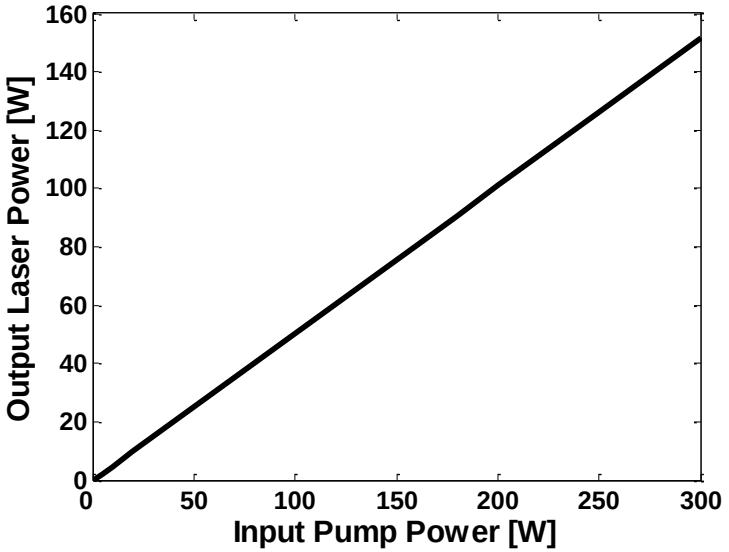

LASER CHARACTERISTIC

Thermal effects : variation of the refractive index, cladding modes more bounded by increasing temperature, lens effect

100W LASER PUMP at 920 nm
Yb1200 20/400DC

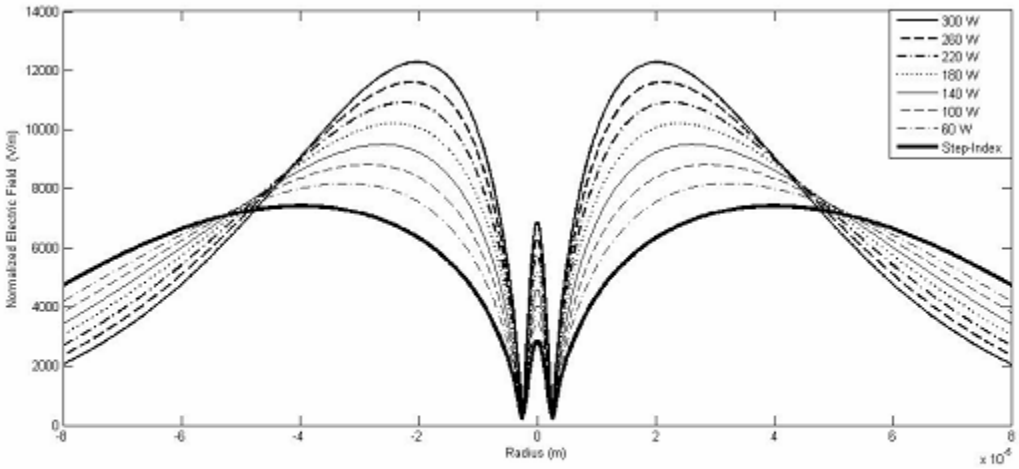

Thermal effects on fundamental DC mode

Cooperation
SHIRAZ University – Iran

M. SABAEIAN, H. NADGARAN, M. DE SARIO, L. MESCIA AND F. PRUDENZANO: "Thermal effects on double clad octagonal Yb:Glass fiber laser". - Optical Materials, 2009.

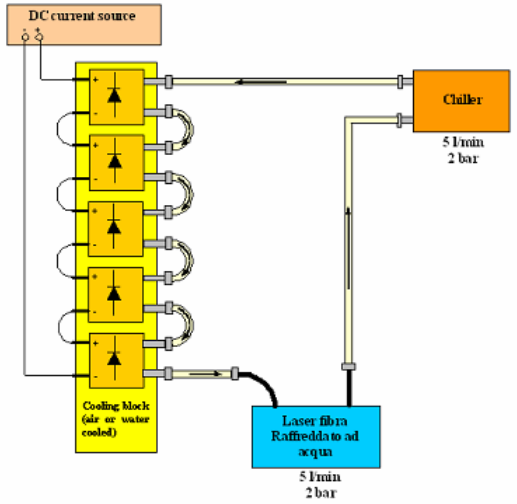

Water cooling system

- Chiller Termotek-AG.
- n. 5 laser diodes Pearl nLight (50 W)
- Power supply SM120-13 da 1500 W
- Ccooling plate for pump laser diodes Pearl della nLight
- Chiller TERMOTEK-AG P310-16728-AW-A-T (da 750W)
- Ytterbium doped fiber Yb1200 20/400DC
- MM Combiner 6 input ports
- 2 mirror Bragg reflector gratings
- 2 Passive fibre

Output Cable with collimator, S/N: 8616)

- Colder connectors: Colder NS4D17006 (3/8 Hose Barb Valved In-Line Coupling Body), Colder NS4D22006 (3/8 Hose Barb Valved In-Line Coupling Insert)

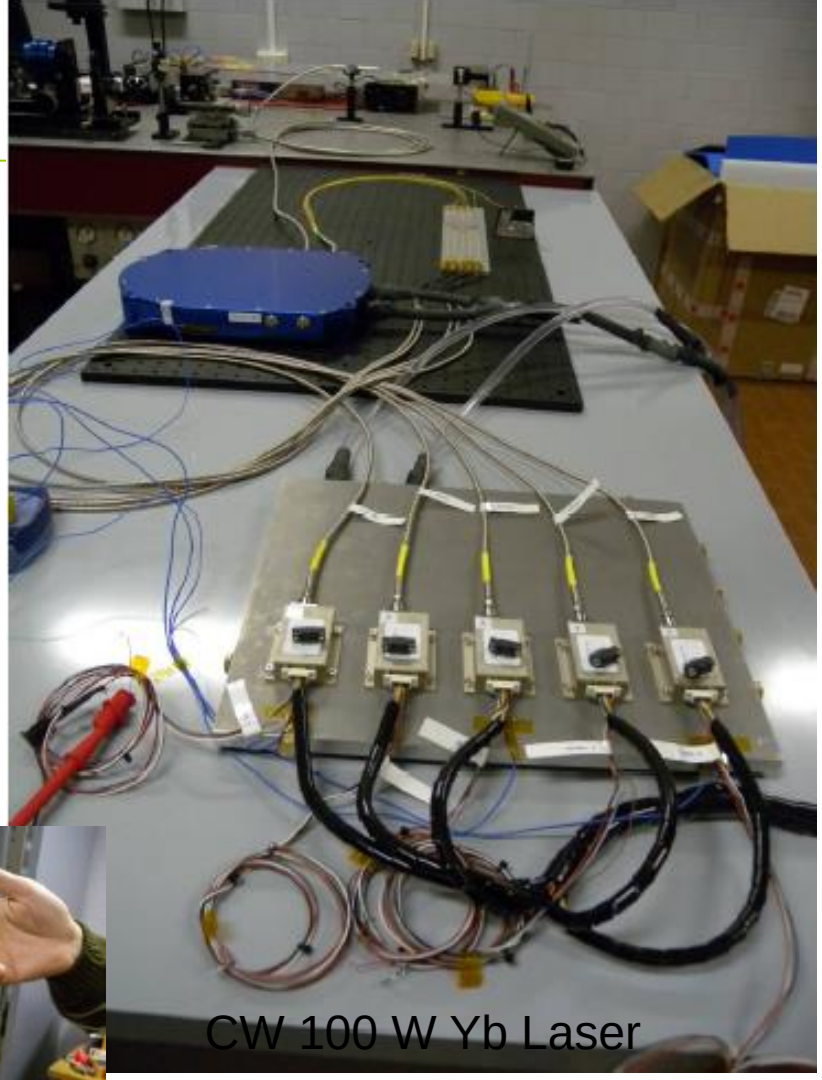

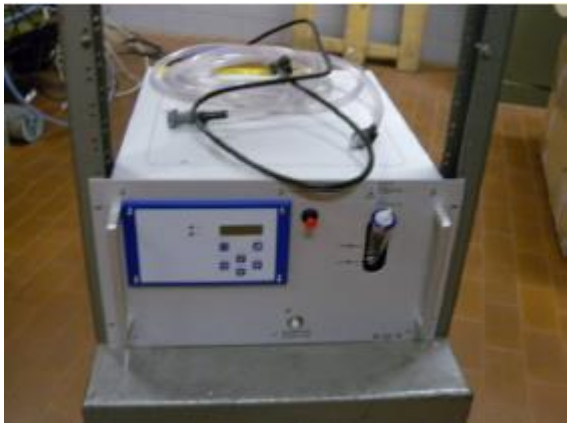

Chiller TERMOTEK-AG P310-16728-AW-A-T - 750W.

Power supply DELTA ELEKTRONIKA BV SM120-13, 1500 W.

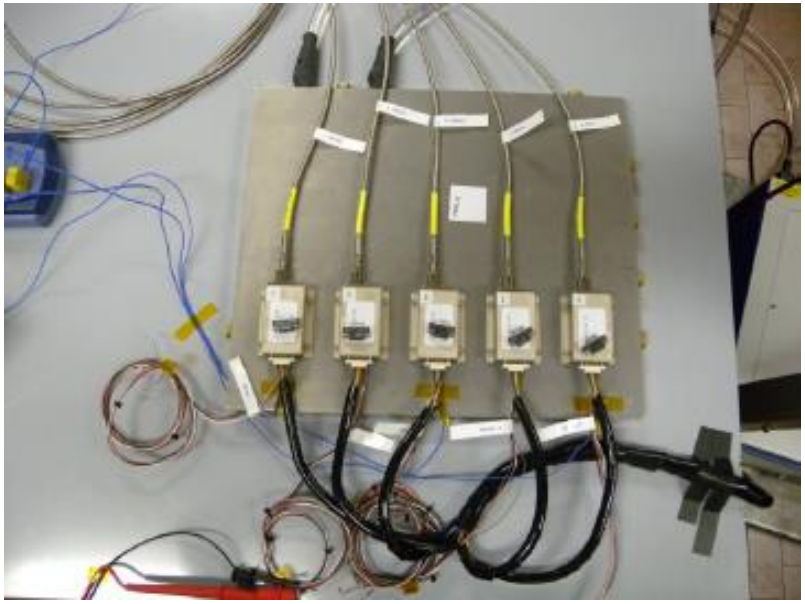

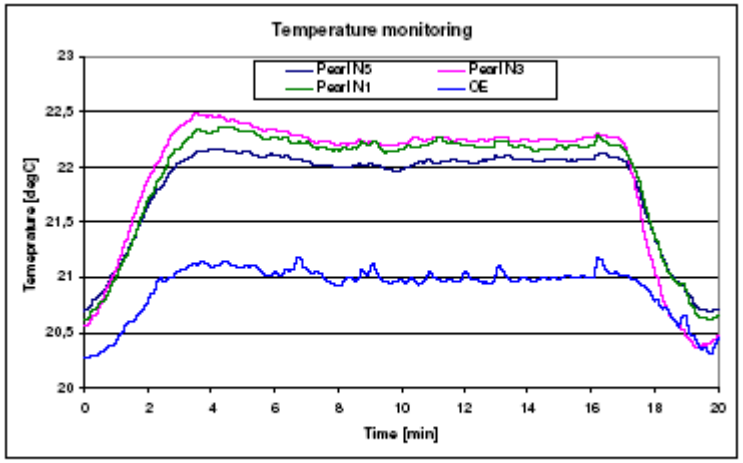

Figure 15 Short term test results

Thermal behaviour of the pump laser diodes and OE versus time

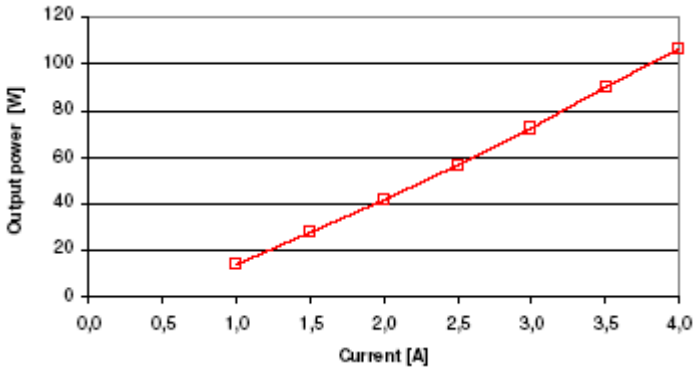

Output power versus the supply current

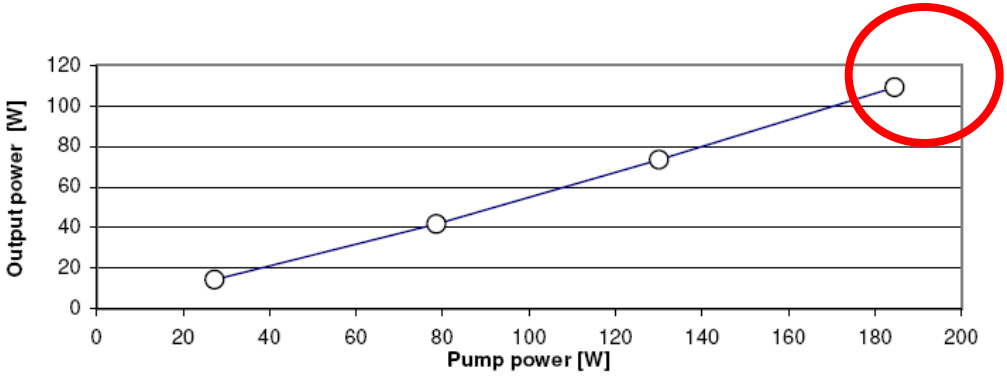

Laser output power versus pump power [W]

Tab. laser efficiency

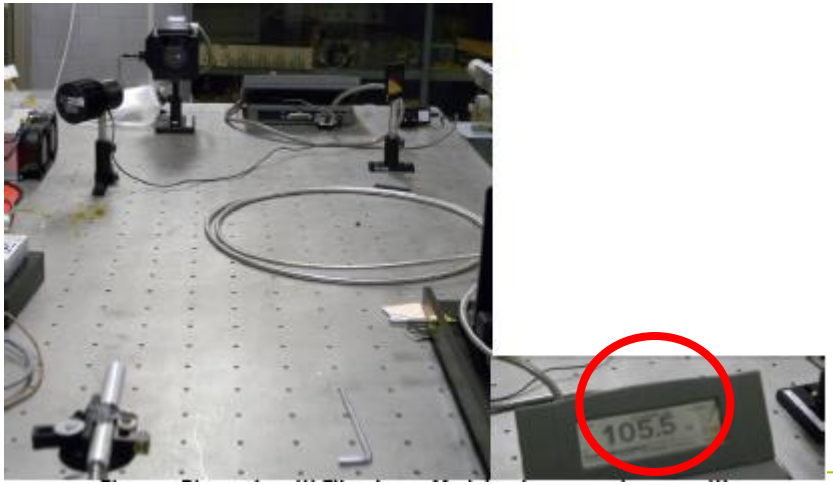

I[A]	Pump power [W]	OE power [W]	Optical-optical efficiency [%]
0,5	N/A	1,02	N/A
1	27,34	14	51,2 %
1,5	52,97	27,5	51,9 %
2	78,6	41,5	52,8 %
2,5	104,35	56,3	54,0 %
3	130,1	72,3	55,6 %
3,5	157,35	89,7	57,0 %
4	184,6	105,9	57,4 %

Figure 5 Output power vs. current

110 W emission and high beam quality in single transverse mode , electrial-optical efficiency $\eta \cong 36\%$.

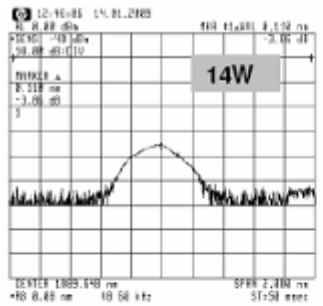

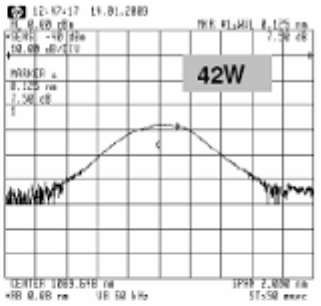

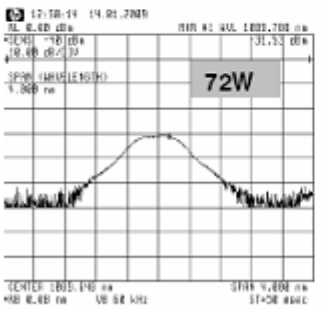

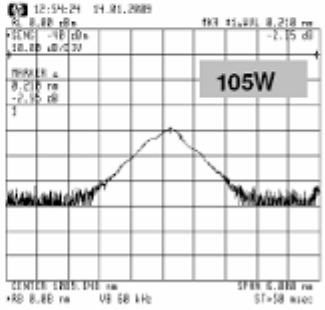

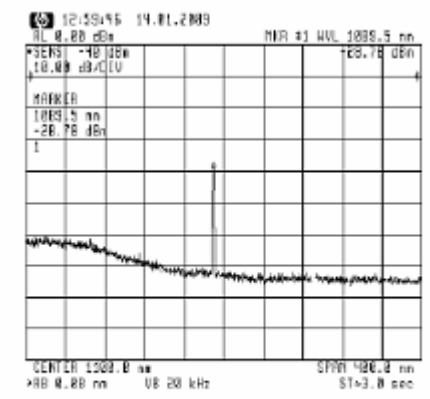

Output laser spectrum, measured at 14W, 42W, 72W, 105W, peak at λ=1089.5nm, FWHM= 0.42 nm at 105W.

Mid-IR fiber laser

- Thulium (Tm^{3+}) and Holmium (Ho^{3+}), 2 μm wavelength.
- Ytterbium Yb^{3+} and Tm^{3+} or ions can be used as sensitizer in Ho^{3+} doped glasses.
- Erbium Er^{3+}-doped Zr-Ba-La-Al-Na (ZBLAN), wavelength range from 2.65 to 2.85 μm.
- Erbium-Praseodymium Er^{3+}-Pr^{3+} co-doped ZBLAN fiber lasers, **3 μm wavelength**.
- Dysprosium Dy^{3+}-doped chalcogenide glass, **4.5 μm wavelength.**
- Er^{3+}-doped $Ga_5Ge_{20}Sb_{10}S_{65}$ chalcogenide, **4.5 μm wavelength.**

S. D. Jackson, A. Sabella, A. Hemming, S. Bennetts, and D. G. Lancaster: A high power 83W holmium-doped silica fiber laser operating with high beam quality, Opt. Lett., vol. 32, no. 3, pp. 241–243, 2007.
F. Auzel, D. Meichenin, and H. Poignant: Laser cross section and quantum yield of Er at 2.7 μm, Electron. Lett., vol. 24, no. 15, pp. 909–910, Jul. 1988.
X. Zhu and R. Jain: Compact two-Watt wavelength-tunable Er:ZBLAN mid-IR fiber laser, Opt. Lett., vol. 32, pp. 2381–2383, 2007.
P. S. Golding, S. D. Jackson, T. A. King, and M. Pollnau, "Energy transfer processes in Er -doped and Er-Pr -codoped ZBLAN glasses," Phys. Rev. B, vol. 62, no. 2, pp. 856–864, Jul. 1, 2000.
R.S. Quimby, L.B. Shaw, J. S. Sanghera, I.D. Aggarwal, "Modeling of Cascade Lasing in Dy:Calchogenide Glass Fiber Laser With Efficient Output at 4.5 um", IEEE Phot. Techn. Letters, 20, 2008

Chalcogenide Glass

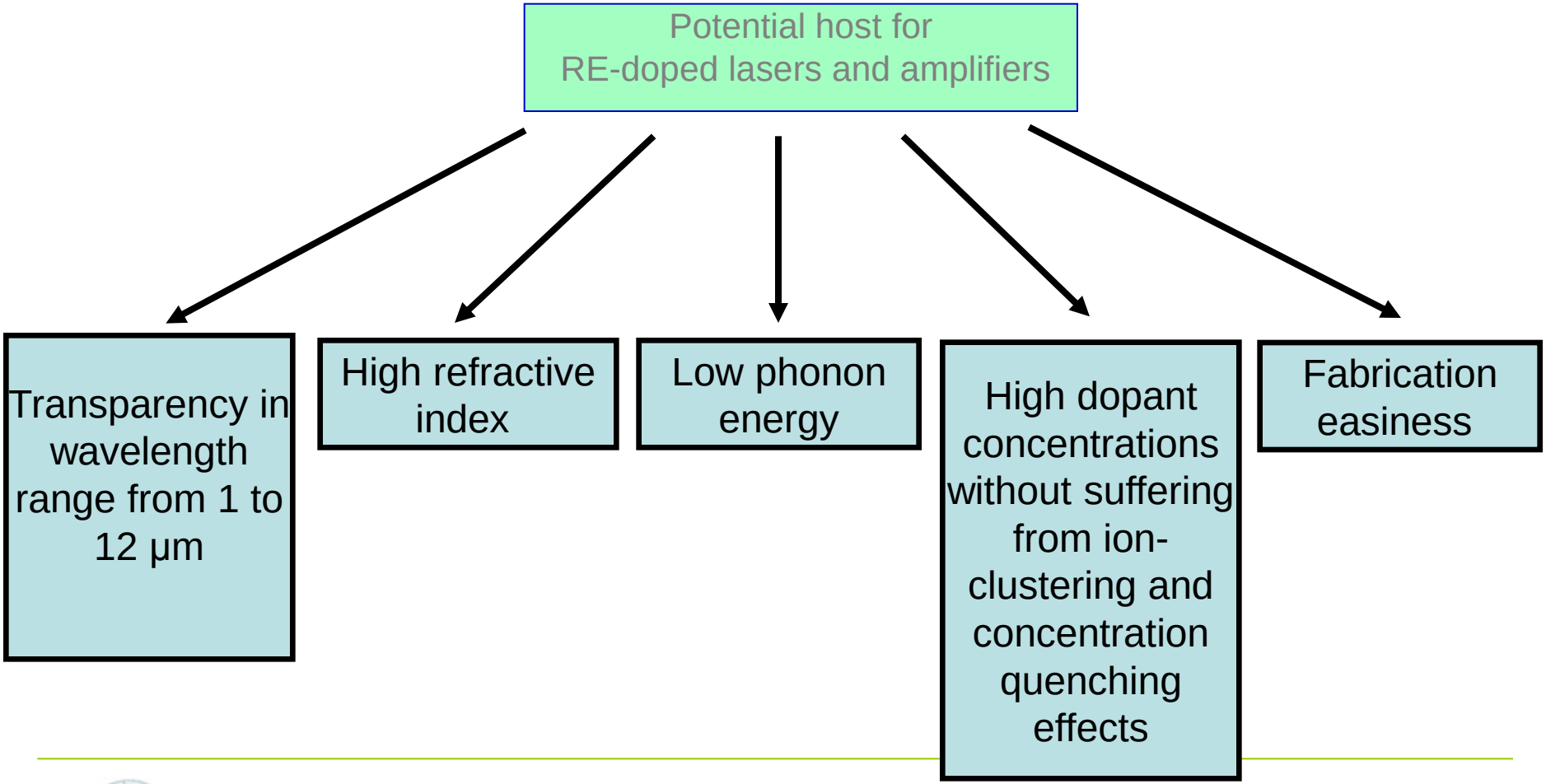

PCF Laser Design

MOF $Ga_5Ge_{20}Sb_{10}S_{65}$ chalcogenide glass

Gallium Germanium Antimony Sulphur

3 hole rings

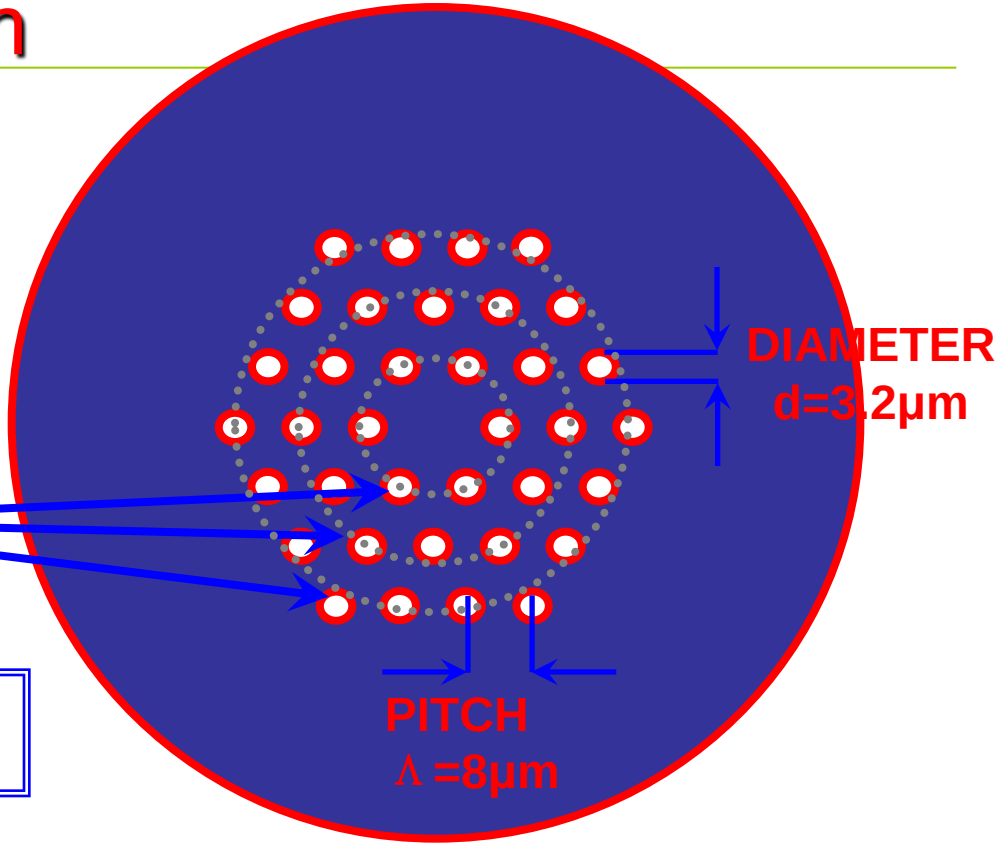

Erbium Concentration N_{Er}=11.53 x 10^{25}ions/m^3

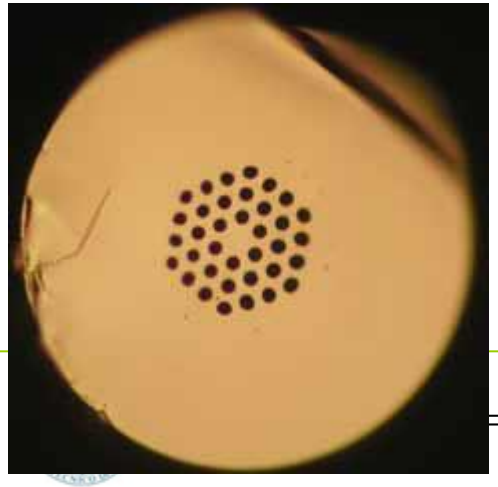

F. Prudenzano, L. Mescia, L. Allegretti, M. De Sario, T. Palmisano, F. Smektala, V. Moizan, V. Nazabal, J. Troles: "Design of Er3+-doped chalcogenide glass laser for MID-IR application" J. Non-Crystalline 2009

λ=4.5µm

Fabrication of LPG/FBG in PCF

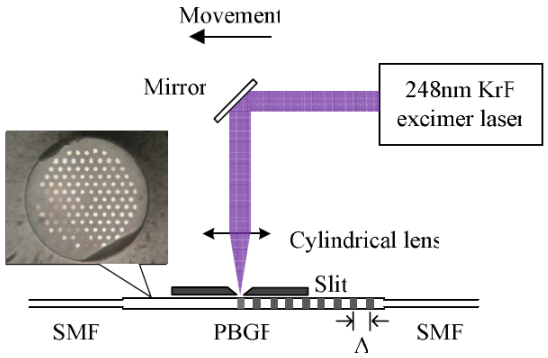

Fig. 2 Schematic setup for LPG inscription in all-solid PBGFs. Inset, microscopic image for the cross section of the PBGF.

L. Jin, Z. Wang, Y. Liu, G. Kai, X. Dong," Ultraviolet-inscribed long period gratings in all-solid photonic bandgap fibers", 2008 / Vol. 16, No. 25 / OPTICS EXPRESS

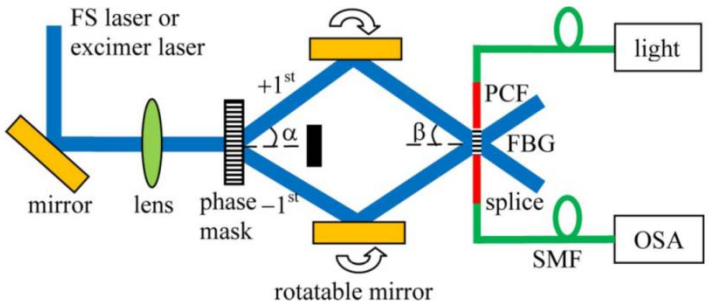

Fig. 1. (Color online) Scheme of experimental setup for inscribing FBGs with two-beam interference and a femtosecond laser or an excimer laser.

Y. Wang, H. Bartelt, M. Becker, S. Brueckner, J. Bergmann, J. Kobelke, M. Rothhardt," Fiber Bragg grating inscription in pure-silica and Ge-doped photonic crystal fibers", l2009 / Vol. 48, No. 11 / APPLIED OPTICS

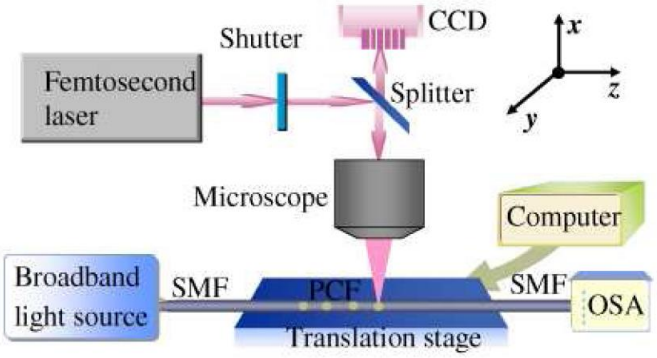

Fig. 1. Experiment setup for LPG fabrication.

S. Liu, L. Jin, W.Jin, D. Wang, C. Liao, Ying Wang," Structural long period gratings made by drilling micro-holes in photonic crystal fibers with a femtosecond infrared laser", 15 March 2010 / Vol. 18, No. 6 / OPTICS EXPRESS

Fiber Gratings

Device applications

- Optical filtering
- Mode conversion
- Sensing (strain, temperature, refractive index …)
- Gain flattening
- Wavelength tuning
- Suppression of amplified spontaneous emission

Fiber Bragg gratings FBGs

Coupling occurs between modes travelling in opposite directions

Long period gratings LPGs

Coupling occurs between modes travelling in the same direction

A suitable LPG to enhance the pump power absorption, at wavelength λ_p=980 nm is designed.

Transverse electric field profiles at the pump wavelength, λ = 980 nm.

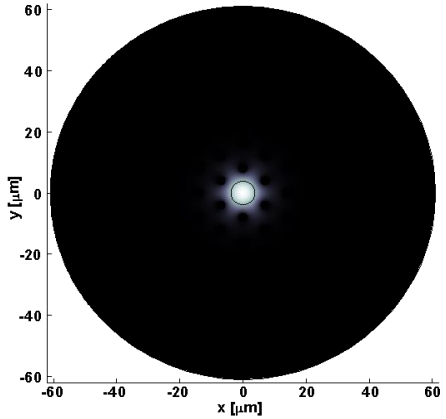

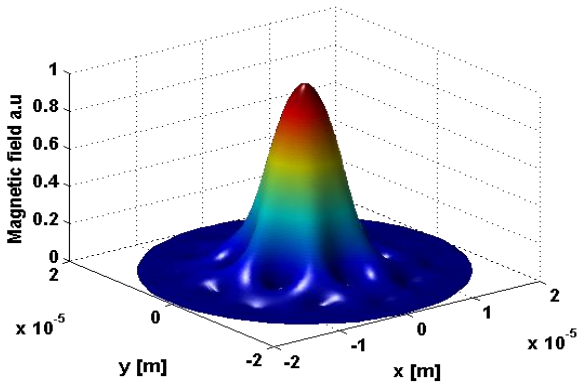

Core fundamental mode HE_{11}

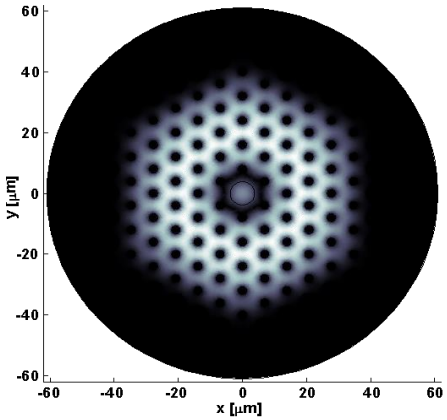

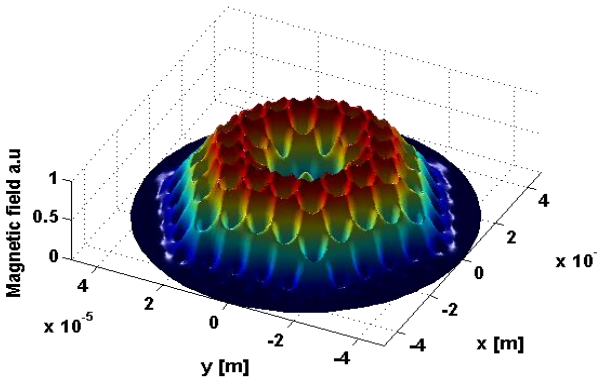

(a) Inner cladding mode HE^{cl}_{11}

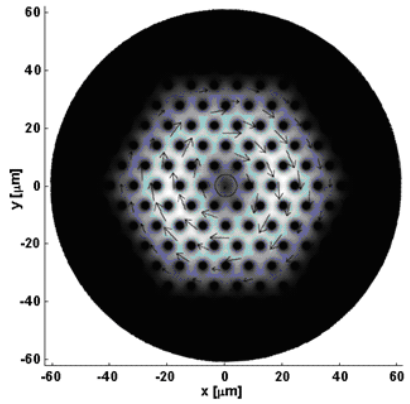

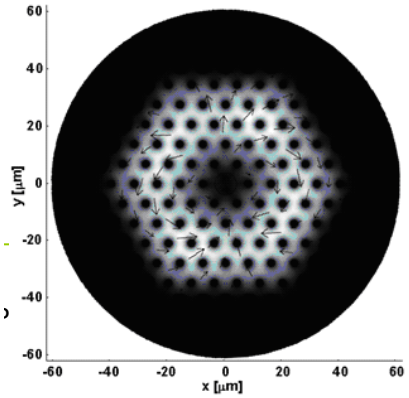

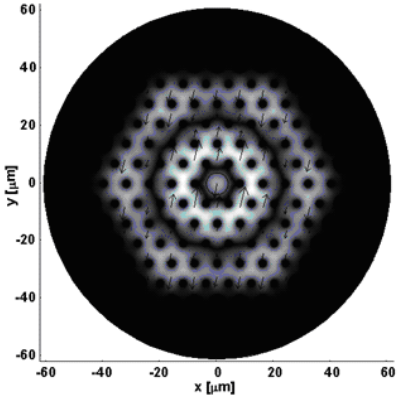

Inner cladding modes
(b) TE^{cl}_{01}-like
(c) EH^{cl}_{11}-like
(d) HE^{cl}_{12}-like

LPG Long-Period Grating

Simulated results with an home made computer code based on coupled mode theory

Optimization of pump absorption in MOF lasers via multi-long-period gratings: design strategies

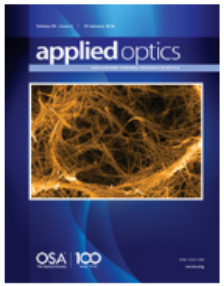

Francesco Prudenzano, Luciano Mescia, Tommaso Palmisano, Michele Surico, Marco De Sario, and Giancarlo Cesare Righini

Applied Optics Vol. 51, Issue 9, pp. 1420-1430 (2012) • https://doi.org/10.1364/AO.51.001420

G. Calò, A. D'Orazio, M. De Sario, L. Mescia, V. Petruzzelli, L. Allegretti, T. Palmisano, F. Prudenzano: "Improvement of the Pump Power Coupling in Double Cladding Photonic Crystal Fiber," 2008 IEEE/LEOS Winter Topical Meeting Series, 14-16 January 2008, pp. 146-147, Sorrento, Italy 14-16 January 2008, ISBN 978-1-4244-1595-3.

SKETCH OF THE SENSOR

Segment C is equal to sect.A, it is an Ytterbium doped laser. The optical cavity is obtained by employing to fiber Bragg gratings (FBGs)

sensors

MDPI

Article

Electromagnetic Modelling of Fiber Sensors for Low-Cost and High Sensitivity Temperature Monitoring

William Scarcia, Giuseppe Palma, Mario Christian Falconi, Francesco de Leonardis, Vittorio M. N. Passaro and Francesco Prudenzano *

Received: 21 September 2015; Accepted: 23 November 2015; Published: 30 November 2015
Academic Editor: Elfed Lewis

Department of Electrical and Information Engineering, Politecnico di Bari, via E. Orabona n. 4, Bari 70125, Italy; w.scarcia@live.it (W.S.); giuseppe.palma@poliba.it (G.P.); christian.falconi@poliba.it (M.C.F.); francesco.deleonardis@poliba.it (F.L.); vittorio.passaro@poliba.it (V.M.N.P.)
* Correspondence: francesco.prudenzano@poliba.it; Tel.: +39-80-596-3781; Fax: +39-80-596-3410

Abstract: An accurate design of an innovative fiber optic temperature sensor is developed. The sensor is based on a cascade of three microstructured optical fibers (MOFs). In the first one a suitable cascade of long period gratings is designed into the core. A single mode intermediate and a rare-earth activated Fabry-Perot optical cavity are the other two sensor MOF sections. An exhaustive theoretic feasibility investigation is performed employing computer code. The complete set-up for temperature monitoring can be obtained by utilizing only a low cost pump diode laser at 980 nm wavelength and a commercial optical power detector. The simulated sensitivity S = 315.1 μW/°C and the operation range ΔT = 100 °C is good enough for actual applications.

light
m

Segment
multimoda
core mode
cladding
towards th

F the
not
arger

THE DE
MEAS

ON

(a)

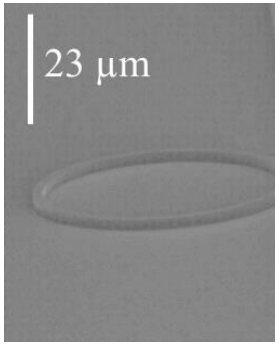

FIG. 1 – SEM images
a ridge waveguide on a s
waveguide fab

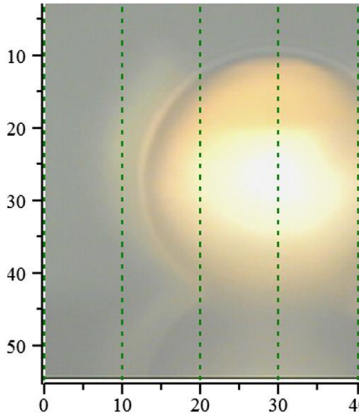

Optical microscope and SEM
coated with Au/Pd conductive

Research Article | Vol. 24, No. 23 | 14 Nov 2016 | OPTICS EXPRESS 26956
Optics EXPRESS

Novel double step approach for optical sensing via microsphere WGM resonance

G. PALMA,[1] M. C. FALCONI,[1] F. STARECKI,[2] V. NAZABAL,[2] T. YANO,[3] T. KISHI,[3] T. KUMAGAI,[3] AND F. PRUDENZANO[1,*]

[1]*Department of Electrical and Information Engineering, Politecnico di Bari, Bari 70125, Italy*
[2]*Institute des Sciences Chimiques de Rennes, UMR 6226, Université de RENNES 1-CNRS, Rennes 35042 Cedex, France*
[3]*Department of Chemistry and Materials Science, Tokyo Institute of Technology, Tokyo 152-8550, Japan*
**francesco.prudenzano@poliba.it*
https://www.moe-group.it

Abstract: The use of resonant whispering gallery modes (WGMs) for sensing exhibits various drawbacks and critical points related to the microsphere and tapered optical fiber fabrication tolerance. The uncertainty on the fiber taper and microsphere geometry or the gap between the microsphere and the fiber taper can complicate or limit the actual use of these devices for sensing, requiring peculiar calibration of the WGM based sensing set-up. An alternative double-step approach is proposed in this paper. In particular, the geometrical parameters of the set-up are recovered preliminarily and then the rare earth parameters are recovered via simple transmittance/gain measurements. The method is based on a refined electromagnetic model of the device suitably integrated with a particle swarm optimization (PSO) approach. The percent errors made on the up-conversion coefficients C_{up} and C_3 are extremely low, being 0.75%, 0.05%, respectively. The procedure is very robust. It can be applied more in general, allowing the sensing of other physical parameters via simple transmittance measurements instead of wavelength shift ones, in both microsphere and microbubble based set-up.

l, A.
enide
otical

3D model integrated with PSO

Layout scheme of spherical microresonator

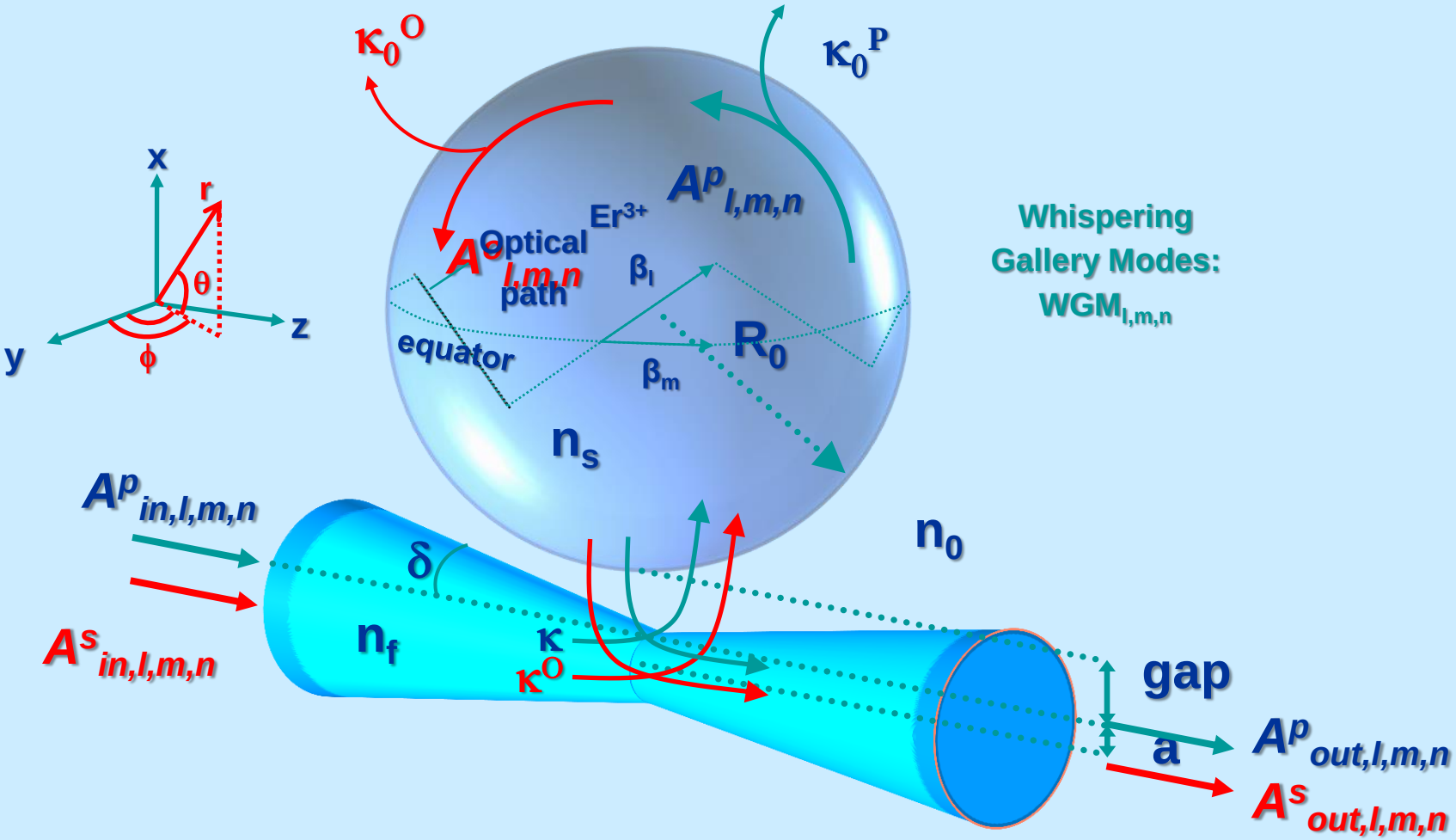

Politecnico di Bari

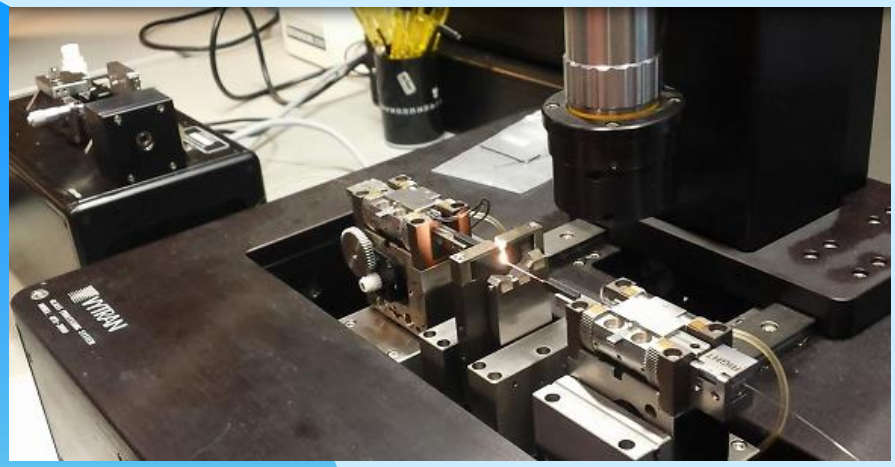

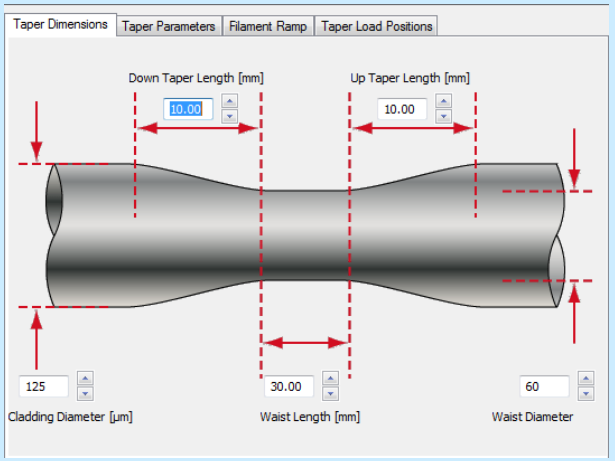

OPTICAL TECHNOLOGIES

Optical components, that may be employed in a variety of microwave photonics applications, are successfully fabricated with the GPX-3400 Vytran, such as tapers and multicombiner.

At right the results of the measurement made on a taper with a spatial reduction ratio from 125 μm to a waist of 60 μm, total length of 98.00 mm is reported. A maximum power loss of 0.96 dB and a minimum power loss of 0.46 dB are achieved, showing very good performance in terms of power loss.

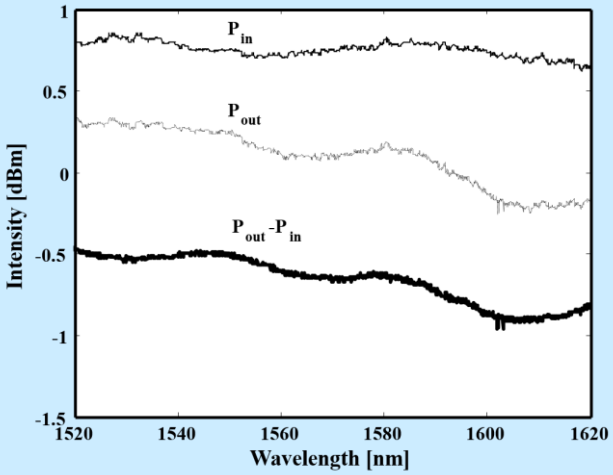

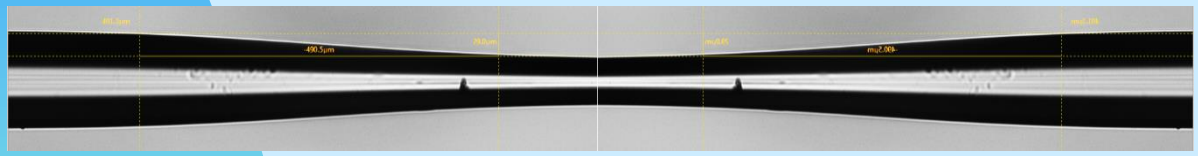

OPTICAL TECHNOLOGIES

tapering.mp4

Three tapers having different shape and size are measured following this simple procedure. The light from a tunable laser source is coupled into the taper and the signal coming from the other end of the taper is collected and analyzed by an optical spectrum analyzer.

splicing -reale.avi

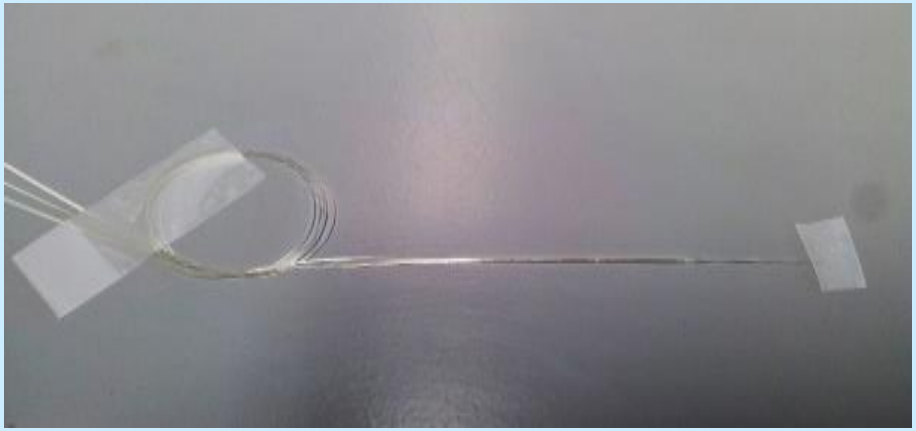

From left in clockwise:

- Optical spectrum analyzer
- Glass Processing System GPX-3400
- Vytran with Automatic Cleaver LDC-400
- Vytran
- Optical Bench
- Fiber Recoater PTR-200 Vytran

Optical bench, optical spectrum analyzer, optical sources are used for optical characterization.

francesco.prudenzano@poliba.it

Cooperation on fiber optics

"Verres& Céramiques" - Prof. V. Nazabal and Prof.F. Starecki

Tokyo Institute of Technology Prof. Yano

Fonctions Optiques pour les Technologies de l'informatiON prof. L. Bodiou e J. Charrier

Istituto di Fisica Applicata "Nello Carrara", CNR-IFAC – dott. Nunzi Conti

.....Nottingham University, Swansea University, Fyla....

- **FIB-LAS-2004.07: Sviluppo e applicazioni di laser a fibra ottica. Progetto FAR. Art. 5 D.L. 297/99**
- **PON02_00576 _3329762 DD MIUR n.818/Ric. del 26/11/12**
- **HORIZON 2020 - COST ACTION MP 1401, Advanced Fibre Laser and Coherent Source as tools for Society, and Lifescience**
- **Galileo 2007 UIF "Modellizzazione e fabbricazione di prototipi di dispositivi ottici innovativi per i sistemi di comunicazione ad elevate prestazioni"**